"Physics of Combustion Of New Oxidizer/Polymer Mixtures"

Final Technical Report (Item 0001AD)
by
Anatoli A. Zenin

October, 2003

United States Army

EUROPEAN RESEARCH OFFICE OF THE U.S. ARMY

London, England

CONTRACT NUMBER N62558-02-M-6022

Russian Academy of Sciences,
Semenov Institute of Chemical Physics

REPORT DOCUMENTATION PAGE			Form Approved OMB No. 0704-0188
1. AGENCY USE ONLY	2. REPORT DATE **22 October 2003**	3. REPORT TYPE AND DATES COVERED **Final Report: 22 August 2002 - 22 October 2003**	
4. TITLE AND SUBTITLE **"Physics of Combustion of New Oxidizer/Polymer Mixtures"**			5. FUNDING NUMBERS C
6. AUTHOR **Anatoli A. Zenin**			
7. PERFORMING ORGANISATION NAME AND ADDRESS **Semenov Institute of Chemical Physics**, Russian Academy of Sciences Kosygin Street 4, 119991 Moscow, Russia			8.PERFORMING ORGANISATION REPORT NUMBER -
9. SPONSORING/MONITORING AGENCY NAME AND ADDRESS **Mr. KEVIN LINDEN** U.S. Naval Regional Contracting Center, Det. London, Government Buildings, Block 2, Wing 12, Lime Grove, Ruislip, Middlesex HA4 8BS England Telephone: 4 (0)208 385 5390; Fax: 4 (0)208 385 5348; E-mail: KEVIN.LINDEN@NRCC-LONDON.NAVY.MIL			10. SPONSORING/MONITORING AGENCY REPORT NUMBER
11. SUPPLEMENTARY NOTES			
12a. DISTRIBUTION/AVAILABILITY STATEMENT DISTRIBUTION STATEMENT A Approved for Public Release Distribution Unlimited			12b. DISTRIBUTION CODE

13. ABSTRACT

Combustion of mixtures of CL-20 (hexanitrohexaazaisowurtzitane - HNIW) with thermoplastics BAMO-AMMO, and GAP, and mixtures of GAP/HMX and (BAMO-AMMO)/HMX is investigated by methods of thermocouple technique in a bomb of constant pressure at sample temperature and pressure variations. The main burning wave parameters are determined. Macrokinetics of gasifications are evaluated and positions of burning rate control stages are established. Temperature and pressure sensitivities of burning rates and surface temperatures were found, and criteria of stable combustion were estimated. Burning rate response functions to oscillatory pressure in linear and nonlinear approximations were found, and influence of elevated pulsating pressures was estimated. Thus, full characterization of the investigated mixtures at stable and pulsating combustion was made. Obtaining « sequence of preferences » for the studied mixtures allows the best (preferable) mixtures to be established. Conclusion contains descriptions of characteristic features of combustion mechanisms of the mixtures on base of CL-20 and HMX, at stable and pulsating pressures. Recommendations for future works are suggested.

14. SUBJECT ITEMS	15. NUMBER OF PAGES
Combustion mechanisms, CL-20 (HNIW), HMX, mixtures of GAP/HNIW, (BAMO-AMMO)/HNIW, GAP/HMX, (BAMO-AMMO)/HMX, pressures, sample temperatures, temperature profiles, parameters of burning waves, heat manifestations in zones, limiting stages, combustion stability, pressure and temperature sensitivities, pressure and burning rate pulsations, linear and nonlinear response functions to oscillatory pressure.	37
	16. PRICE CODE NTIS

17. SECURITY CLASSIFICATION OF REPORT	18. SECURITY CLASSIFICATION OF THIS PAGE	19 SECURITY CLASSIFICATION OF ABSTRACT	20. LIMITATION OF ABSTRACT
UNCLASSIFIED	UNCLASSIFIED	UNCLASSIFIED	UL

Body of the Report

(1). 1. Tasks of the Report.

The Final Report (item 000AD) must include a statement of the problem studied, and a summary of the most important results, received in the interim reports. The Report must contain burning rate and surface temperature sensitivities of the studied mixtures (having energetic binders on the base of new oxidizer CL-20 (HNIW), and mixtures having HMX) to pressure and initial temperature, burning rate response functions of the mixtures to linear and nonlinear pulsations. Information about experimental arrangements and the obtained temperature profiles and burning wave parameters at pressure and sample temperature variations must be suggested also. Conclusions about combustion mechanisms of the studied mixtures under stable and pulsating conditions must be made and recommendations for future work must be suggested.

2. Objects of Investigations.

The following mixtures of binder/oxidizer were used in the investigations:
1) GAP/HNIW, 2) (BAMO-AMMO)/HNIW, 3) GAP/HMX, and 4) (BAMO-AMMO)/HMX. Characteristics of ingredients were as follows: HNIW (CL-20) is a polycyclic caged nitramine, which have the chemical nomination - 2,4,6,8,10,12-hexanitrohexaazaisowurtzitane; it is a powder with cristal particles of density ρ=2,01 gr/cm^3; the particles have nonregular shape and sizes from 1 up to 150 μm; HMX particles have sizes less than 200 μm; GAP is an energetic binder, polyglycidyl azide, with molecular weight about 2000 and element content $C_{36,7}H_{5,2}O_{16,9}N_{41,6}$; energetic binder (BAMO-AMMO) is a copolymer of two thermoplastic elastomers - poly bis 3,3-azidomethyloxetane (BAMO) and poly 3-azidomethyl-3-methyloxetane (AMMO), in proportion 50:50.
Characteristics of the mixtures were as follows:
1. GAP/HNIW, ratio 20:80, sum formula $O_{23,93}H_{21,05}N_{27,96}C_{17,01}$; density ρ=1,78 gr/cm^3, adiabatic (thermodynamic) temperature at 10 MPa is T_{ad}=2927°C.
2. (BAMO-AMMO)/HNIW, ratio 20:80, sum formula $O_{24,2}H_{22,4}N_{27,94}C_{17,21}$; ρ=1,76 gr/cm^3, adiabatic temperature at 10 MPa is T_{ad}=2934°C
3. GAP/HMX, ratio 20:80, sum formula $O_{23,63}H_{31,7}N_{27,67}C_{16,86}$; ρ=1,74 gr/cm^3, T_{ad}=2420°C at 10 MPa.
4. (BAMO-AMMO)/HMX, ratio 20:80, sum formula $O_{23,9}H_{33,05}N_{26,95}C_{17,21}$; ρ=1,72 gr/cm^3, T_{ad}=2404°C at 10 MPa.

3. Microthermocouple Techniques and Experimental Arrangements.

Temperature profiles of the combustion waves and burning surface temperatures were measured by microthermocouple methods. Ribbon U-shaped thermocouples made of alloys W+5%Re/W+20%Re of 2-7 μm thick were imbedded into the samples. Cylindrical samples of the mixtures (8 mm in diameter and 3 cm in length) were burned in window bomb (volume 2000 cm^3) of constant pressure in atmosphere of gas nitrogen. The samples with 2-3 thermocouples had been ignited by electrically heated wire; thermocouple signals were recorded by amplifier and oscillograph. The samples were burned in a bomb of constant pressure in atmosphere of nitrogen at pressures 0.1 (1.0) -10 MPa and at sample initial temperatures T_o= -100, +20, and +100°C. Burning rates were measured by determination of time delay between the thermocouple signals, by microfilming of sample combustion and by determination of time of pressure increase during the sample combustion (pressure change was measured by Kisstler pressure detectors). Burning surface temperatures were measured by thermocouples that are being pressed to the surface during sample combustion and by establishing locations of slope breaks on temperature profiles, recorded by the thermocouples (there is the theory and experimental substantiation of burning surface temperature measurements by determination of temperature of the break).

The theory of thermocouple measurements in combustion waves of solids shows that all requirements of the theory meet in thesee investigations. Different types of metal wires for thermocouples were used (We,Re and Pt,Rh) to test the catalytic effect on thermocouples. This catalytic effect was not observed.

4. Results of The Measurements.

The investigated mixtures burned at different pressures (0.5 – 10 MPa) and at sample temperatures T_o from –100 up to 100°C, as a rule relatively steady, without periodically pulsations of burning rate. Mixture GAP/HNIW can burn also at 0.1 MPa.

4.1. Carbon residue. Carbon residue produces on the burning surface of mixtures on the base of CL-20 at decreased pressures. The residue in mixture GAP/HNIW has increased density (up to 0.05 g/cm^3 at 0.1 MPa) and holds shape of the sample after going of the burning wave at pressures 0.1 - 2 MPa. The density of the residue decreases at pressure increasing: it is about 0.01-0.02 g/cm^3 at 0.5 -2 MPa. The residue, which holds the shape of sample, is a carbon lattice, through which gaseous combustion products blow easily. At pressures 2-8 MPa the carbon residue during combustion of GAP/HNIW has forms of carbon flakes, which amount decreases with pressure and at 10 MPa the residue doesn't observed. In combustion waves of mixture (BAMO-AMMO)/HNIW the carbon residue at low pressures has form of carbon flakes and at elevated pressures the residue doesn't observed. Carbon residue on the burning surface of the mixtures 3, 4 (on the base of HMX) did not observed. Variation of T_o doesn't influence on the carbon residue production.

Results of experimental measurements of mass burning rates and burning surface temperatures in combustion waves of the mixtures show Tables 1 - 4, which contain averages values of these parameters for every combustion regime.

4.2. Mass burning rates **m**. Tables 1, 2 show that burning rates of mixtures on base of HNIW are very high and that burning rates of mixture 1 are significantly lower than the rates of mixture 2. Indeed burning rates of mixture 1 in pressure interval 0.5-10 MPa comprise 0.5-4.0 g/cm^{2}c (T_o=20°C), but those of mixture 2 - 0.8 - 6.9 g/cm^{2}c. It can be seen from Tables 1 - 4 that burning rates of mixtures on the base of HNIW are significantly higher than the rates of mixtures on the base of HMX. Indeed, burning rates of mixtures 3, 4 in interval 0.5-10 MPa change from 0.1 up to 1.25-1.45 g/cm^{2}c (T_o=20°C). It is important to stress, that influence of type of binder on burning rate of HNIW-based mixtures is significantly higher than that on burning rate of HMX-based mixtures.

It was established at sample temperature variations, that burning rates of mixture 2 at negative sample temperatures have especially significant changing and because of that the burning rates were obtained at -50 and -100°C - see Table 2.

Standard deviation of m measurements is about ±5 %.

4.3. Burning surface temperatures **T_s**. Tables 1 and 2 show that burning surface temperatures T_s of mixtures 1 and 2 are significantly lower than surface temperatures of mixtures 3 and 4. Indeed the surface temperatures of mixture 1 comprise 248-355°C (0.1-10 MPa), and T_s of mixture 2 comprise 285-382°C (0.5-10 MPa), wheras surface temperatures of mixture 3 comprise 330-492°C and 330-500°C, correspondingly (T_o=20°C). It can be seen, that, in spite of large burning rates of mixtures on the base of HNIW, the surface temperatures of these mixtures significantly lower than values of T_s of mixtures on the base of HMX, having small burning rates.

Standard deviation of T_s measurements is about ±5 %.

4.4. Temperature profiles. Temperature distributions T(x) along combustion waves of the investigated mixtures have irregular temperature pulsations. These pulsations are significant at 0.1-2 MPa, possibly due to carbon residue creation and carbon flakes tearing off from the burning surface. However, at p>2 MPa the temperature profiles are relatively smooth. 5-8 numbers of temperature profiles T(x) were obtained for every combustion regime and then averaged curves of T(x) were obtained. Figures 1-7 present typical averaged temperature profiles T(x), in solid and gas, at different pressures and sample temperatures for mixture 1. Similar averaged temperature profiles have other mixtures (see Interim Report item 001AC). Peculiarities of the main burning wave parameters of the mixtures can be seen from Tables

1 - 4. The figures and Tables show that all mixtures have in the gas phase a two-zone structure of the profiles at middle pressures, beginning approximately from 0.5 MPa. This two-zone structure (low-temperature, or first zone, and flame zone) exists up to about 2 MPa. Mixture 1 can burn at 0.1 MPa and at this pressure the gas phase of this mixture contains only one low-temperature zone. At elevated pressures, beginning from 2-6 MPa, both zones merge into one zone of the gas phase for all mixtures at all sample temperatures.

Detailed measurements of temperature profiles at negative sample temperatures were performed. Mixtures 1, 3, and 4 have increased irregular temperature pulsations at T_o= -100°C. Mixture 2 showed more regular temperature pulsations at T_o= -100°C at p<5 MPa. It gives some base for suspicion that combustion of this mixture under indicated condition has unstable character.

5. The Experimental Data Processing.

The processing of the obtained temperature profiles allows a set of burning wave parameters to be determined. Tables 1-4 present the dependencies of the parameters on pressure and T_o. Table 5 shows estimated due to gas product content the dependencies of coefficients of heat conduction λ_g and specific heat c_p of the gas phase on temperature.

5.1. Temperature and geometric characteristics of temperature distributions in gas.

Values of mean temperature of the first zone, T_1, for mixture 1 are equal to 800-1200°C and for mixture 2 - 1000-1150°C (T_o=20°C). Temperatures of T_1 for mixture 3 comprise 980-1050°C and for mixture 4 - 900-1020°C. It was estblished that sample temperature variations change T_1 approximately by similar way. Standard deviation of T_1 measurements is about ±10 %.

Flame temperatures T_f for mixture 1 are equal to 2500-2930°C (T_o=20°C) and for mixture 2 - 2200-2930°C (T_o=20°C). Values of T_f for mixture 3 comprise 1900-2420°C and for mixture 4 - 2000-2400°C. It can be seen that flame temperature of mixtures on base of HNIW is much higher than that of mixtures on base of HMX. Maximal flame temperatures T_f were obtained at 5-8 MPa. It was estblished that sample temperature variations change T_f approximately by similar way.

Distances L_1 between the burning surface and the beginning of the flame zone (L_1 is the length of the first flame) decrease when pressure increases. Values of L_1 for mixture 1 are equal to 2- 1 mm (0.1-2 MPa), for mixture 2 - to 1-0.25 mm (0.5-5 MPa), for mixture 3 - to 0.6-0.5 mm (0.5-1 MPa), and for mixture 4 - to 0.5-0.4 mm (0.5-1 MPa) - all for T_o=20°C. It can be seen that mixtures on base of HNIW have greater length of the first flame than mixtures on base of HMX.

Distances L between the burning surface and the flame (up to ~0.99 T_f) also decrease when pressure increases. In fact, L is the length of the gas phase reaction zone. Values of L for mixture 1 are equal to 4-1.8 mm (0.5-10 MPa), for mixture 2 - to 5-2 mm (0.5-10 MPa), for mixture 3 - to 2-1.3 mm (0.5-10 MPa), and for mixture 4 - to 2.2-0.9 mm (0.5-10 MPa) - all for T_o=20°C. It can be seen that mixtures on base of HNIW have larger length of the gas phase reaction zone than mixtures on base of HMX.

Standard deviation of L_1 and L measurements are ±(15-30)%.

5.2. Coefficients of heat diffusivity and heat conduction in solid heat layer.

Coefficients of solid heat diffusivity were obtained by formula $\chi = l \cdot \tau_b$, where l is thickness of heat layer of the condensed phase (see next section). Tables 1 - 4 show that values of χ increase when pressure increases. The values of χ for mixtures 1, 2 increase from $2 \cdot 10^{-3}$ cm^2/s up to $6 \cdot 10^{-3}$ cm^2/s. For mixtures 3, 4 the values of χ comprise $(1.0\text{-}3.8) \cdot 10^{-3}$ cm^2/s. These values are typical ones for χ of solid heat layer of many propellant mixtures.

The coefficients of solid heat conduction were obtained by formula $\lambda_s = \chi \cdot c \cdot \rho$. It was assumed that solid specific heat is equal to c=0.35 cal/g·K for mixtures 1 and 2 and c=0.4 cal/g·K for mixtures 3, 4. Tables 1, 2 show that λ_s increases with pressure, and increases when mean solid heat layer temperature increases. Values of λ_s comprise $(10\text{-}40) \cdot 10^{-4}$ cal/cm·s·K for mixtures 1, 2 and $(7\text{-}26) \cdot 10^{-4}$ cal/cm·s·K for mixtures
3, 4.

5.3. Characteristic sizes in solid and the gas phase.

Characteristic thickness l and l_m in solid, presented on Tables 1-4, were obtained by temperature distributions in the condensed phase. Experimentally obtained thickness of heat layer in solid l is a distance between the burning surface and a section in solid with temperature $T^*=(T_s-T_o)/e + T_o$ (e is the base of ln). Thickness of l_m of the partly melt layer (with melt oxidizer) in the condensed phase is a distance between the burning surface and a section with oxidizer melt temperature T_m. It was assumed that the melt temperature for CL-20 is equal to T_m=190°C and for HMX - T_m=280°C. Tables show that thickness of l and l_m decrease when pressure increases. Values of l_m are always less than values of l, especially for mixtures 3, 4.

Conductive sizes ϑ of the gas phase were obtained by formula: $\vartheta=\lambda_g/mc_p$; where λ_g is coefficient of heat conduction in gas and c_p is coefficient of specific heat of the gas phase. Values λ_g and c_p were estimated by content of combustion products. The obtained dependencies of $\lambda_g(T)$ and $c_p(T)$ are presented on Table 5. Values of λ_g, which were used for ϑ calculations, were taken at temperatures T_1 for two-zone structures and at $T_f/2$ for one-zone structures. Tables 1-4 show that values of ϑ quickly decrease when pressure increases. Values of ϑ comprise 18-1.8 μm for mixtures 1, 2 and 51-4 μm for mixtures 3, 4. It can be seen that always the following inequalities take place: $\vartheta<<L_1$ and $\vartheta<<L$.

Relative thickness of the gas-phase reaction layer were estimated by formula $\Omega=L_1/\vartheta$ MPa for two-zone structures, or by formula $\Omega=L/\vartheta$ for one-zone structures. It can be seen that inequality of $\Omega>>1$ always takes place. It implies that a wide reaction zone in the gas phase is observed for all combustion regimes of combustion of mixtures 1-4.

5.4. Heat manifestations: heat release in solid and heat feedback from gas into solid.

The temperature profiles and burning surface temperatures were used for obtaining heat parameters of the burning waves. Heat flux from gas to solid q·m by heat conduction was estimated by the following formula:

$$q\cdot m=-\lambda_g(T)\cdot(dT/dx)_o; \qquad (5.1)$$

Here: $(dT/dx)_o=\varphi$ is the temperature gradient in gas close to the burning surface. Values of φ were determined by slopes of the temperature distributions T(x) in gas close to the surface.

Heat feedback q from gas into solid by heat conduction was estimated by the following formula:

$$q=-\lambda_g(T)\cdot\varphi/m; \qquad (5.2)$$

Values of λ_g were taken at temperatures $T=T_s+100$°C.

Formula for heat release Q in reaction layer of the condensed phase (or on the burning surface) have the following forms:

for mixtures 1, 2 $\quad Q=c\cdot(T_s-T_o)-q-q_r$; $\qquad (5.3)$

and

for mixtures 3, 4 $\quad Q=c\cdot(T_s-T_o)-q-q_r+q_m$; $\qquad (5.4)$

where q_m is the heat of HMX melting in mixtures 3, 4; heat of HNIW's melting are not known and because of that formula for mixtures 1, 2 don't have member of q_m. Heat of HMX's melting is equal to 24 cal/g (per gram of HMX) and because of that q_m=19.2 cal/g (per gram of mixtures 3, 4). Radiant heat feedback q_r from flame into solid was estimated for all mixtures by using of content of combustion products and real flame thickness of the burning samples in the bomb of constant pressure. The heat radiations of CO_2, H_2O, H_2, etc were taken into considerations. It was assumed that coefficient of heat radiation absorption of the burning surface was equal to 0.5. Tables 1-4 show the obtained heat parameters.

It can be seen from Tables 1-4 that all investigated mixtures have significant positive heat release in solid Q. Parameter Q comprise at pressures 0.5-10 MPa the following values: 60-140 cal/g for mixture 1, 60-140 cal/g for mixture 2, 78-180 cal/g for mixture 3, and 96-185 cal/g for mixture 4. Parameter Q increases always with pressure and decreases with sample temperature increasing. It can be seen that, as a rule, the

values of Q for HMX-based mixtures higher than for HNIW-based mixtures. Temperature gradient φ in gas close to burning surface has significant values $\{(2\text{-}15)\cdot10^{-4}$, K/cm$\}$ and always increases with pressure and decreases with sample temperature increasing. On the contrary, heat feedback q from gas into solid always decreases when pressure increases. Values of q are comparable with values of Q only at low pressure (0.5 MPa) and only for HMX-based mixtures. Under other conditions values of q are significantly smaller than values of Q, especially at elevated pressures. Indeed, Tables 1, 2 show that q comprises in the studied pressure intervals the following values: 11-6.3 cal/g for mixture 1, 9-4.3 cal/g for mixture 2, 64-25 cal/g for mixture 3, and 46-22 cal/g for mixture 4. At last, the values of q_r are small; they comprise: 4-8 cal/g for mixture 1, 2.5-4.6 cal/g for mixture 2, 0.7-3.7 cal/g for mixture 3, and 0.6-4 cal/g for mixture 4. It can be seen, that total heat feedback $q+q_r$ from gas to solid surface less than heat release in solid, i.e. inequality $Q>q+q_r$ always take place.

5.5. Heat release rate in gas close to the burning surface.

Heat release rates W_o in gas close to the surface were estimated by using of the obtained data. W_o shows, obviously, the intensity of chemical reactions in gas. Values of W_o were obtained by the following expression:

$$W_o=c_p\cdot m\cdot\varphi; \qquad (5.5)$$

This expression was obtained from equation of heat conduction for stable propagating combustion waves for the case of significant positive heat release in solid and wide reaction zone in gas. These experimental facts were established in the previous sections and it implies that the indicated expression for W_o is valid. Values of c_p here were taken at temperatures $T=T_s+100°C$. Tables 1, 2 show that values of W_o quickly increase with pressure. The heat release rate W_o comprise at 0.5-10 MPa the following values: 5-177 kcal/cm^{3}s for mixture 1, 10.8-355 kcal/cm^{3}s for mixture 2, 1.4-64 kcal/cm^{3}s for mixture 3, and 0.9-73 kcal/cm^{3}s for mixture 4 (at $T_o=20°C$). It can be seen that HNIW-based mixtures have more intensive chemical reactions in gas near the burning surface than mixtures on the base of HMX.

5.6. Burning Rate Control Regions.

The results of measurements of parameters $q+q_r$ and Q and the investigations of the gas phase zone behavior show that burning rate of the mixtures are caused by the heat release in solid (or on solid surface) and, in a smaller degree, by the heat feedback from the gas layer which is close to the burning surface. It was mentioned above also that the values of $q+q_r$ decreases when the burning rate increases. These facts show that heat release in solid (or on solid surface) is a main factor of creating of the burning rate of the mixtures. Heat feedback from gas to solid is only small additionăl factor of the burning rate creating and influence of this factor on values of m decreases when pressure increases (at pressures $p\leq10$ MPa). Then, the obtained data, presented in Tables 1 - 4, allow an important conclusion to be made: the high temperature region of the burning waves cannot affect the burning rate. Indeed, the influence of the heat release in the gas phase on the burning rate can be estimated by the following formula obtained as a solution of the heat conduction equation:

$$m\cdot q=\int_0^\infty \Phi(x)\cdot\exp(-x/\vartheta)\cdot dx; \qquad (5.6)$$

This formula shows that influence of heat release in gas (here $\Phi(x)$·is distribution of heat release rate in the gas phase) on m decreases very quickly when $x>\vartheta$. Tables 1-4 show that values ϑ are small and they are significantly smaller than gas zone sizes L and L_1: see large values of Ω for all combustion regimes. That implies that high temperature region of the burning waves cannot affect the burning rate. Thus the obtained results show that the burning rate control regions in the combustion waves for all regimes of the mixtures combustion, under investigated conditions, are the regions of heat release in solid just under the burning surface (or immediately on the burning surface) and thin low-temperature gas layers close to the burning surface (at $x\approx\vartheta$). High temperature gas regions cannot influence the burning rate in fact because of a very large heat resistance of the gas phase of the mixtures.

5.7. Macrokinetics of Solid Gasification.

The following equation connects burning rate of solid with burn-surface temperature and

macrokinetic characteristics of solid gasification:

$$m^2=\lambda_s\rho/Q^2\cdot\Re T_s^2/E\cdot k_o Q^*\cdot 1/N\cdot\exp(-E/\Re T_s); \qquad (5.7)$$

where $N=1/\eta_s+(1-\eta_s)/\eta_s\cdot\ln(1-\eta_s)-(q/Q)\cdot[\ln(1-\eta_s)]/\eta_s$; $\eta_s=Q/Q^*$; Q^* is the maximum of the heat release in solid, E is activation energy of limiting stage of the gasification process, T_s in K. For studied combustion waves $N\cong 1$. The expression was obtained by solution of system of two equations for the steady propagated burning wave (the heat conduction equation for solid phase and the equation of diffusion of reagents were solved). The burning wave propagates due to heat release in solid Q and heat feedback from gas to solid q. Function of the volumetric heat release rate Φ_s in solid reaction layer was assumed as follows:

$$\Phi_s(\eta, T)=Q^*k_o\cdot\rho\cdot(1-\eta)\cdot\exp(-E/\Re T); \qquad (5.8)$$

Here η is the reaction completeness ($\eta=\eta_s$ on the burning surface), k_o is the pre-exponent multiplier. The member $\exp(-E/\Re T_s)$ in the equation above plays the most important role in this formula. Because of that the connection m and T_s can be presented by the following simplified expression:

$$m=A\cdot\exp(-E/2\Re T_s); \qquad (5.9)$$

This expression has been designated "gasification law". The results of measurement, presented in Tables 1, 2, allow the following gasification law for mixtures 1 and 2 (i.e. for mixtures, based on HNIW) to be obtained:

$$m=1.8\cdot 10^6\cdot\exp(-32800/2\Re T_s); \quad (m \text{ in } g/cm^2s,\ T_s \text{ in K}) \qquad (5.10)$$

Possibly, value E=32800 kcal/mole is an activation energy of the limiting stage of the process of oxidizer CL-20 gasification in the reaction layer of mixtures 1 and 2.
The results of measurement, presented in Tables 3, 4, allow the following gasification laws for mixtures 3 and 4 to be obtained:

$$m=1.1\cdot 10^4\cdot\exp(-28000/2\Re T_s); \quad (m \text{ in } g/cm^2s,\ T \text{ in K}); \qquad (5.11)$$
(valid at $T_s<500°C$),

The obtained value of activation energy of the gasification process is very close to that of cyclic nitramines (when $T_s<500°C$). Possibly, gasification of oxidizer HMX in the reaction layer of burning mixtures 3 and 4 is the limiting stage of the process of the mixtures gasification.

6. Pressure and Temperature Sensitivities of Burning Rates and Surface Temperatures and Criteria of Stable Combustion.

6.1. The Pressure and Temperature Sensitivities.

The following pressure and temperature sensitivities for burning rates and burning surface temperatures were found from the data presented on Tables 1-4:

$\beta=(\partial\ln m/\partial T_o)_{p\text{-const}}$, - temperature sensitivity of mass burning rate;

$\mathbf{r}=(\partial T_s/\partial T_o)_{p\text{-const}}$, - temperature sensitivity of burning surface temperature;

$\nu=(\partial\ln m/\partial\ln p)_{To\text{-const}}$, - pressure sensitivity of mass burning rate;

$\mu=(T_s-T_o)^{-1}\cdot(\partial T_s/\partial\ln p)_{To\text{-const}}$, - pressure sensitivity of burning surface temperature;

The obtained results for the investigated mixtures are shown on Tables 6 for $T_o=20°C$. The Table also contains parameter **k**, which was found by formula $\mathbf{k}=\beta\cdot(T_s-T_o)$.

It can be seen that burn-rate pressure sensitivities ν for mixture 1 increase with pressure : parameter ν is equal to 0.37-0.6 at pressures 0.1-2 MPa, and ν=0.8-0.93 at pressures 5-10 MPa. Mixture 2 has

increasing values of ν at 0.5-2 MPa (ν=0.55-0.82) and decreasing ν at p>2 MPa (ν=0.73-0.68). Parameter ν decreases with pressure for mixtures 3 and 4 from ν=0.83-0.9 at 1 MPa to ν=0.76-0.79 at 10 MPa.
It can be seen, that burn-rate pressure sensitivities ν for HMX –based mixtures, as a rule, are higher than ν for HNIW-based mixtures (an exclusion for values of ν for mixture 1 at p>5 MPa, which are extraordinary high).
Standard deviation of values ν determinations is ± (1-3%).

Temperature sensitivity of mass burning rate β has a typical dependence on pressure: a maximum at 0.5-2 MPa and decreasing with pressure increasing. Values of β are close each other for mixtures 1, 3, 4. Indeed, β=0.23-0.28 %/K at 1 MPa and decreases to 0.12-0.17 %/K at 10 MPa for the mixtures. Values of β for mixture 2 are much higher than that of other mixtures. Indeed, β=0.3 %/K at 1 MPa, 0.36 at 2 MPa and 0.28 at 10 MPa.
Standard deviation of values β determinations is ± (5-6%).

Parameters of k for mixtures 1, 3, 4 are less, than 1 at all pressures, only for mixture 2 at $p \geq 2$ $k > 1$. Very low values k has mixture 1: $k \leq 0.6$ at 1-10 MPa.
Standard deviation of values k determinations is ± 10%.

Temperature sensitivity of surface temperature r for HMX-based mixtures 1 has decreasing dependence on pressure and comprise r=0.17-0.19 at 1 MPa and decreases to r=0.09-0.067 at 10 MPa. Mixture GAP/HNIW has lower values of r: this parameter is almost constant in pressure interval 0.1-10 MPa and comprises 0.06-0.1. Mixture (AMMO-BAMO)/HNIW has increasing dependence of r on pressure and this parameter is equal to 0.13 at 0.5 MPa and increases to 0.2 at 10 MPa. Mixture 2 has maximal values of r at p > 2 MPa.
Standard deviation of values r determinations is ± 10%.

Pressure sensitivities of burning surface temperature μ for HMX-based mixtures are close each other and comprise 0.16-0.17 at 1 MPa and decrease to 0.09 at 10 MPa. HNIW-based mixtures have other dependencies for μ on pressure: parameter μ of mixture 2 practically independent on pressure and comprises 0.1-0.12, and μ of mixture 1 increases from 0.06 at 0.1 MPa to 0.14 at 10 MPa.
Standard deviation of values μ determinations is ± (1-3%).

The obtained sensitivities are the most important characteristics of combustion processes of solid mixtures. These characteristics are used for characterizations of solid mixtures at stable and at pulsating combustion. The obtained above sensitivities allow ones to show that well-known jacobian $\delta = \nu \cdot r - \mu \cdot k$ is very close to zero. Indeed, accuracy of δ obtaining is about ±0.005, and it is inside of experimental accuracy of the determination. **It implies that equation (5.9) has experimental validation.**

Estimation of criteria of stable combustion (see next section) is the second example of usage of the sensitivities for determination of region of stable combustion.

6.2. Criteria of Stable Combustion.

The simplest criterion of stable combustion is Zeldovich's criterion $\mathbf{k}=\beta \cdot (T_s - T_o)$. It is used, when surface temperature is changing no significantly at pressure and sample temperature variations. The criterion predicts the stable combustion at $\mathbf{k} < 1$. However, practically always, the significant changing of the surface temperature takes place (see Tables 1-4). In this case at $\mathbf{k} > 1$ (at $k < 1$ Zel'dovich's and Novozhilov's criteria are identical) Novozilov's criterion $\mathbf{k^*}$, which takes into consideration T_s changing, must be used. The criterion predicts stable combustion at $\mathbf{k^*} < 1$. The formula for the criterion is as follows:

$$\mathbf{k^*}=(k-1)^2/(k+1)r\ ; \qquad (6.1)$$

Calculated criterion **k** for the investigated mixtures shows Table 6. It can be seen that mixtures 1, 3, and 4 have $k < 1$. It shows that these mixtures have stable combustion under indicated conditions. Further estimations showed that even at T_o= -100°C mixtures 1, 3, and 4 have stable combustion because for these mixtures $\mathbf{k^*} < 1$ at all investigated sample temperatures (at T_o = -100°C) mixtures 1, 3, and 4 have $k > 1$ at low pressures).
Table 6 shows that at T_o=20°C mixture (AMMO-BAMO)/HNIW has $\mathbf{k} > 1$ at pressures 2-10 MPa.

But estimations of **k*** values show that this mixture has also stable combustion even at $T_o \geq -50°C$ – see Table 7. However, at $T_o = -100°C$ and $p < 5$ MPa for mixture 2 inequality $\mathbf{k^*} > 1$ takes place. It implies that at $T_o = -100°C$ and $p < 5$ MPa mixture (AMMO-BAMO)/HNIW burns unstable. This conclusion confirms results obtained for temperature profile measurements - see above, section *4.4*.

7. Second Step of Data Processing : Combustion Characterizations at Pulsating Pressure

7.1. Pressure-Driven Burn-Rate Response Functions at Linear Approximation.

The obtained results, which were received at constant, nonpulsating pressures, allow us to study burning rate behavior of the investigated mixtures under conditions of oscillatory pressure. It can be made due to obtained above sensitivities for m and T_s. This paragraph is devoted to this study.

Let us assume that external pressure changes by harmonic way and is equal to :

$$p=p_o+p_1\cdot\cos\varpi t, \qquad (7.1)$$

here p_o is a constant mean pressure level and p_1 is an oscillating pressure ($p_1<<p_o$), t is current time, and ϖ is cyclic frequency of oscillation in 1/s.

Then mass burning rate in linear approximation is equal to:

$$m=m_o+m_1\cos(\varpi t+\psi)\,; \qquad (7.2)$$

where m is current burning rate, m_o is stationary burning rate at pressure p_o , m_1 is a pulsating burning rate ($m_1<<m$), and ψ is phase shift.

Then dimensionless burning rate has the following form:

$$V=1+V_{10}\cos(\varpi t+\psi), \qquad (7.3)$$

here $V=m/m_o$, $V_{10}=m_1/m_o$.

It is convenient to analyze burning rate response in complex form. In this case complex dimensionless burning rate is equal to $V=1+V_{10}\cdot e^{-i\omega t}$ and complex dimensionless pressure is equal to $\eta=1+\eta_1\cdot e^{-i\omega t}$, where $\eta_1=p_1/p_o$, and ω is dimensionless frequency.

The following expression for burning rate response function to harmonic oscillatory pressure at linear approximation takes place:

$$U = [\nu + (\nu\cdot r - \mu\cdot k)\cdot(z - 1)]/[1 + r\cdot(z - 1) - k\cdot(z - 1)/z]; \qquad (7.4)$$

Here $z=(1+\sqrt{1+4i\omega}\,)/2$; $U=V_{10}/\eta_1$, V_{10} is dimensionless burning rate complex amplitude, and ω is dimensionless frequency, which is equal to the cyclic frequency ϖ, in 1/s, multiplied by the time of solid heat layer relaxation χ/r_b^2. Values of ν, μ, k and r here are based on the mean pressure p_o and because of that data from Table 6 can be used for estimations of complex functions of U. Thus, indeed, we can study the burning rate behavior of the investigated mixtures under conditions of pulsating pressure. The equation (7.4) is based on the supposition that relaxation time of solid heat layer is much longer that those for reaction layer of solid and the leading part of the gas phase. Estimations show that for the investigated mixtures this supposition is valid: values of χ/r_b^2 are at least 10-20 times higher than other relaxation times. Because of that, all estimations of the response functions were made for dimensionless frequency interval ω=0-20.

Typical dimensionless amplitudes Re{U}of burning rate response functions and phase of the response, Im{U}, in radians, as dependencies on ω are shown on Figures 8-14 for mixture 1. Similar functions were obtained for other mixtures. Peculiarities of characteristics of the functions show Table 8 (see below). It can be seen that the real part of $U(\omega)$ may reach values, which are much greater than its steady state value $Re\{U(0)\}=\nu$. It is a consequence of high quality (in filter theory terminology) of our oscillatory systems. The maximum of Re{U} is at a frequency, which are close to the natural (resonance)

frequency $\omega_n=\sqrt{k}$ /r. In this frequency area the denominator of equation (7.4) is less than unity. Thus, any small perturbations of the pulsating system can significant influence the response function. It is natural, that function Im{U(ω)}, presenting the phase shift of the response function, changes the sign at the resonance frequency.

Table 8 shows results of calculations of characteristic points of Re{U} and Im{U} for the studied mixtures. Relative standard deviations of values $Re\{U\}_m$ obtaining are ± (10-30%).

The used denominations in Table 8 are as follows:

$Re\{U\}_m$ is maximum of $Re\{U(\omega=\omega_n)\}$ in interval ω =0-20; ω_n - dimensionless frequency, corresponding to this maximum (the resonance frequency); $Re\{U\}_{20} = Re\{U(20)\}$; $Im\{U_{m+}\}$ - maximum of Im{U} in interval ω =0-ω_n, i.e. in positive region of values of ImU; ω_{im} - dimensionless frequency, corresponding to this maximum; $Im\{U_{m-}\}$ - minimum of ImU (if this minimum takes place) in negative region of ImU;

Table 8 shows that response functions Re{U(ω)} for HNIW-based and for HMX-based mixtures weakly depend on ω, especially at elevated p. The result shows that resonance phenomena in the studied burning mixtures are significantly depressed due to viscous behavior of the oscillations. In fact, the pulsating combustion of the mixtures is an example of a relatively smoothed resonance phenomenon.

Table 8 shows, that changing of oxidizer HMX to oxidizer HNIW in mixture with binder GAP, improves pulsating behavior of burning rate. Indeed, mixture GAP/HMX has $Re\{U\}_m$=1.28-1.56, and mixture GAP/HNIW has $Re\{U\}_m$=0.8-1.3. The obtained result is very important, because previous investigations showed that increasing of energy of mixtures leads, as a rule, to deterioration of pulsating behavior of burning rate. But GAP/HNIW has higher energy, than GAP/HMX. So, HNIW in mixture GAP/HNIW demonstrates exceptions to this rule. It is an advantage of the new oxidizer in mixture GAP/HNIW.

On the contrary, mixture (AMMO-BAMO)/HNIW has increased, in comparison with mixture (AMMO-BAMO)/HMX, values of $Re\{U\}_m$. Indeed, mixture 2 has $Re\{U\}_m$=1.2-2, i.e. high response. But mixture 4 has $Re\{U\}_m$=1.2-1.6. Thus, binder (AMMO-BAMO) doesn't suitable for using HNIW as an oxidizer with binder AMMO-BAMO, at any rate without catalytic additives.

So, mixture 1 is the best mixture, having smallest linear response of burning rate on acoustic pressure pulsations; mixture 4 occupies the second place, on the third place stands mixture 3, and the worst one is mixture 2. This situation for values $Re\{U\}_m$ of the studied mixtures in linear approximation can be presented as following « sequence of preferences » :

[GAP/HNIW] < [(AMMO-BAMO)/HMX] < [GAP/HMX] < [(AMMO-BAMO)/HNIW] – LIN. (ℵ)

On the left side here stands the minimal response and on the right side – the maximal one. Mark 'LIN' show, that it is the linear case. It is interesting to note, that difference [$Re\{U\}_m$ – υ] also corresponds to inequality (ℵ).

7.2. Pressure-Driven Burn-Rate Response Functions at Nonlinear Approximation. The Second Order Interactions.

This section introduces the definition of response function of the higher orders. In a common case the acoustic field contains several harmonics (modes). No linearity of combustion process can give the oscillation of the burning rate with different frequencies by interaction of two (or several) other modes. The simplest, and more significant, are the following cases:

1) Interaction of the first and the second harmonics gives the second order correction to linear response function for the first and third harmonics (because the product $\cos\omega\tau$ x $\cos2\omega\tau$ contains oscillations with ω and 3ω frequencies),
2) Self-interaction of the first mode gives the second mode (because the product $\cos\omega\tau$ x $\cos\omega\tau$ contains oscillations with 2ω frequency),

Such nonlinear interaction may produce a significant effect in the case when one of interacting harmonics is close to the natural frequency ω_n.

Values of ν, μ, k and r here are based also on the mean pressure p_o, as in the linear case.

In the next sections for nonlinear approximations the italic letters were used for the same parameters: ν, μ, k, r, p_o, p, p_1.

7.2.1. The second order interaction of the first and the second harmonics.

It was mentioned above, that acoustic field contain in a common case several harmonics. For the second order interactions of the harmonics we must use the following expressions:

$$p=p_o+p_1\cos\omega\tau+p_2\cos(2\omega\tau+\psi); \qquad (7.5)$$

$$m=m_o+m_1\cos(\omega\tau+\psi_{m1})+m_2\cos(2\omega\tau+\psi_{m2}); \qquad (7.6)$$

After presenting of the expressions for dimensionless pressure and burning rate in complex forms and solving of the no stationary heat-conduction equation in the condensed phase, the following solution can be obtained for linear response function plus nonlinear correction of the function by the second order interaction of the first and second modes:

$$V_1 = U + U_{12}\cdot\eta_{12}\eta_2/\eta_1; \qquad (7.7)$$

where : U – linear response function, see eq.(7.4), and $U_{12}\cdot\eta_{12}\eta_2/\eta_1$ is the member of the nonlinear correction. Here :

$$U_{12}=\frac{g_1}{1+r(z\ -1)-k(z-1)/z};\quad \eta_{12}=\eta_1;\quad \eta_1=p_1/2p_0;\quad \eta_2=\frac{p_2\exp(\psi\cdot i)}{2p_0};$$

$$z=(1+\sqrt{1+4i\omega})/2;\quad i=\sqrt{-1};\quad p_1=0.1\cdot p_0;(\#)\qquad \delta=\nu\cdot r-\mu\cdot k;$$

$$g_1=U_1U_2\{g_2+[zr(1-\varepsilon)-1+r(1+\varepsilon)]\}+\nu[U_1(2z_2-2z-1)+U_2z-z_1-1];\quad D=k+r-1;$$

$$g_2=\frac{(z_2-z)i}{2\omega}(D-\frac{k}{z\cdot z_2})+(z_2-z_1)(D-\frac{k}{z\cdot z_2});\quad z_1=(1+\sqrt{1-4i\omega})/2;\quad z_2=(1+\sqrt{1+8i\omega})/2;$$

$\varepsilon=4\Re T_s/E$; where E is activation energy of gasification, and T_s is burning surface temperature under stable combustion at pressure p_0. Functions U_1 and U_2 can be found by eq.(7.4), in which function z must be substituted by z_1 and z_2, correspondingly.

It is important to stress the new aspect of the problem: the complex response function V_1 depends on the phase shift ψ between the first and the second harmonics. Because of that the result of calculations was received for four values of ψ : $0, \pi/2, \pi$, and $3\pi/2$.

The calculated typical nonlinear amplitudes $Re\{V_1\}$ of burning rate response functions and phase shift of the response, $Im\{V_1\}$, as dependencies on ω are shown on Figures 52-22 for mixture 1. Similar functions were obtained for other mixtures. Table 9 shows values of $Re\{V1\}_m$ and ω_n (as $\frac{Re\{V_1\}_m}{\omega_n}$) of the functions. Values of ω_n here are also the resonance frequency, corresponding to $Re\{V1\}_m$.
Relative standard deviations of values $Re\{V_1\}_m$ obtaining are about ± (20-40%).

It can be seen, that nonlinear correction of response functions strongly depends on mixture and on phase shift ψ. At ψ=0: values of $Re\{V_1\}_m$ for mixtures 1 and 4 are close to linear $Re\{U\}_m$ of these response functions practically at all studied pressures. The values of mixture 3 a bit more than linear values, but mixture 2 has a very large increasing of $Re\{V_1\}_m$ in comparison with linear $Re\{U\}_m$ of this mixture. At $\psi=\pi/2$: values of $Re\{V_1\}_m$ for all mixtures even less, than values of linear $Re\{U\}_m$.
At $\psi=\pi$: values of $Re\{V_1\}_m$ always more than linear $Re\{U\}_m$ for all mixtures, but that difference for mixtures 1, 4 and 3 it is not large. However, for mixture 2 it is significant. At $\psi=3\pi/2$: values of $Re\{V_1\}_m$ have maximal values at every pressure. However, for mixtures 1, 3 and 4 they are not very large, but for mixture 2 they are very large: for example, at 2 MPa $Re\{V_1\}_m$=3.38, when linear $Re\{U\}_m$=0.84.

Thus, influence of ψ has no monotonic character: $Re\{V_1\}_m$ increases with phase shift at ψ=0, π and $3\pi/2$, but at $\psi = \pi/2$ values of $Re\{V_1\}_m$ are small for all mixtures, and even less than values of linear $Re\{U\}_m$. It implies, that the response at $\psi = \pi/2$ partly compensates responses at other values of phase shift (because phase shift goes through interval 0-2π).

Values of ω_n here are also strongly depending on ψ. As a rule, values of ω_n at ψ=0 and $3\pi/2$ significantly higher, than those at linear approach, but at $\psi = \pi/2$ and π the values about two times less, than at linear case.

The final conclusion of the section is as follows: the presented data for values of $Re\{V_1\}_m$ show, that the obtained for linear case "sequence of preferences" in section 7.1 is valid also for the second order interaction of the first and second modes.

7.2.2. The second order self-interaction of the first harmonic.

Obviously, for the second order self-interaction of the first harmonic we have the same equations (7.5), (7.6). After presenting of the expressions for dimensionless pressure and burning rate in complex forms and solving of the no stationary heat-conduction equation in the condensed phase, the following solution can be obtained for linear response function plus nonlinear correction of the function by the second order self-interaction of the first mode:

$$V_2 = U_2 + U_{11} \cdot \eta_1^2/\eta_2; \qquad (7.8)$$

where: U_2 – a linear response function, calculated by eq.(7.4), in which z was substituted by z_2, and $U_{11} \cdot \eta_1^2/\eta_2$ is the member of nonlinear correction, i.e. a result of second order self-interaction of the first harmonic. Here:

$$U_{11} = \frac{G_1 + G_2 + G_3}{1 + r(z-1) - k(z-1)/z}; \quad \eta_1 = p_1/2p_0; \quad \eta_2 = \frac{p_1 \exp(\psi \cdot i)}{2p_0}; \quad \delta = \nu \cdot r - \mu \cdot k;$$

$$z = (1+\sqrt{1+4i\omega})/2; \quad i = \sqrt{-1} \quad p_1 = 0.1 \cdot p_0; (\#) \quad z_2 = (1+\sqrt{1+8i\omega})/2; \quad D = k + r - 1;$$

$$G_1 = U^2 \frac{i}{\omega}(z_2 - z)(D - k/z_2 z); \; G_2 = \frac{U^2}{2}\{r[z+1-\varepsilon(z-1)]-1\}; \; G_3 = \nu \cdot U \cdot [1 + \frac{i}{\omega}(z_2 - z)];$$

$$\varepsilon = {}^{4\Re T_s}/_{E}; \qquad \text{Function } U \text{ can be calculated by eq.(7.4).}$$

The response function (7.8) also depends on phase shift ψ, and the calculations also was made for four values of ψ : 0, $\pi/2$, π, and $3\pi/2$.

The calculated typical nonlinear amplitudes $Re\{V_2\}$ of burning rate response functions and phase of the response, $Im\{V_2\}$, as dependencies on ω are shown on Figures 23-30 for mixture 1. Similar functions were obtained for other mixtures. Table 10 shows values of $Re\{V_2\}_m$ and ω_n (as $\frac{Re\{V_2\}_m}{\omega_n}$) of the functions. Relative standard deviations of values $Re\{V_2\}_m$ obtaining are about ± (20-40%).

It can be seen, that second order self-interaction of the first harmonic gives a very small corrections to linear $Re\{U\}_m$ for all investigated mixtures and for all phase shifts ψ. Only effect of decreasing of values ω_n in two times is observed. It is a natural consequence of self-interaction of the first mode.

So, the analysis of this section also show, that "sequence of preferences" is observed also for the second order self-interaction of the first mode.

7.2.3. Increased level of pulsating pressures.

The calculations of previous paragraphs 7.2.1 and 7.2.2 were performed at small amplitude of pressure pulsations: $p_1 = 0.1 \cdot p_0$. It is important, from scientific and practical points of view, to estimate the influence of increased level of pulsating pressures on the obtained nonlinear response functions. It can be made, because the level of pressure pulsations is included in the calculations in evident form: - see above (#). Of course, assumption of small amplitudes of p_1 is the base of the theory of nonlinear response

functions, and because of that the estimations at increased pulsating pressures may give only a tendency of the influence on the response functions. In this section we are estimating this tendency.
Calculations by formulas (7.7) and (7.8) were made at pulsating pressure $p_1 = 0.3 \cdot p_0$ and $p_1 = 0.6 \cdot p_0$. The results of estimations are shown on Tables 9 and 10.
It can be seen, that influence of increased p_1 on the second order self-interaction of the first harmonic doesn't large. Indeed, the increased p_1 gives at the self-interactions, as a rule, about 10% increase of $\mathrm{Re}\{V_2\}_m$ values, and doesn't change the character of the response functions. Influence of pressure amplitude $p_1 = 0.3 \cdot p_0$ on the second order interaction of the first and second modes is more significant. Indeed, the increased p_1 gives here, as a rule, increased values of $\mathrm{Re}\{V_1\}_m$ on about 20-60%, but also without principal changing of character of functions $\mathrm{Re}\{V_1(\omega)\}$ and $\mathrm{Im}\{V_1(\omega)\}$.
Thus, we can conclude, that influence of elevated oscillating pressures doesn't change the main result of section 7 about "sequence of preferences": it is valid also for elevated pulsating pressures:

[GAP/HNIW]<[(AMMO-BAMO)/HMX]<[GAP/HMX]<[(AMMO-BAMO)/HNIW] – NONLIN (ℵ)

On the left side here, as above, stands the minimal response and on the right side – the maximal one. Mark 'NONLIN' show, that it is the nonlinear case with inclusion of the case of elevated oscillating pressures.

So, we can conclude that linear approach to the problem of response function of the investigated mixtures is a good approach, and nonlinear approach, including elevated pulsating pressure level, gives only not large numerical corrections, without principal changing of the main results.

8. CONCLUSIONS

Main Features of Combustion Mechanisms of the Studied Mixtures At Pressure and Sample Temperature Variations and Under Conditions of Stable and Oscillating Pressures.

1) A significant difference in burning rates of mixtures on base of HNIW and on base of HMX takes place: burning rates of HNIW-based mixtures are significantly higher.
2) Influence of type of binder on burning rate of HNIW-based mixtures is significantly higher than that on burning rate of HMX-based mixtures. (AMMO-BAMO)/HNIW mixture has higher burning rate than that of GAP/HNIW mixture. (AMMO-BAMO)/HNIW mixture has also especially high burn-rate temperature sensitivities at negative sample temperatures.
3) Temperatures of burning surface of HNIW-based mixtures are significantly less than those of HMX-based mixtures at all investigated pressures and sample temperatures.
4) Both type of mixtures have two-zone structure of temperature profiles in the gas phase at middle pressures.
5) Both type of mixtures have wide zone reaction in the gas phase and distributed (along the zone) the functions of heat release rate at all investigated pressures and sample temperatures.
6) Significant heat release in solid, increasing with pressure, and relatively small heat feedback from gas to solid due to conduction and radiation, decreasing with pressure, are observed for both type of mixtures.
7) Burning rate control regions in the combustion waves of both mixtures are placed on the burning surface and in the gas phase close to surface, at low temperatures; high temperature gas regions cannot influence the burning rate at all investigated pressures and sample temperatures. Both mixtures have stable combustion under investigated conditions. Intensity of chemical reactions in the gas phase close to the burning surface for HNIW-based mixtures is significantly higher than the intensity for HMX-based mixtures.
8) The investigated mixtures have different macrokinetic laws of solid gasifications, depending on oxidizer and practically independent on binder. Activation energy of HNIW-based mixture gasification is equal to 32.8 Kcal/mole and that of HMX-based mixtures - 28 Kcal/mole (at T_s<500°C).
9) Pressure-driven burn-rate response functions, obtained for the studied mixtures at linear and nonlinear approximations for the second order interactions, have complex character and they are typical for many

condensed systems. The obtained results allow one to establish the best and the worst mixtures, from point of view of the reaction of burning rate on pressure pulsations: the best mixture has the smallest burning rate response and the worst mixture – the largest one. The reaction was established by values of $Re\{V\}_m$ - of the real part of the response functions for the studied mixtures. On the base of the values, the following « sequence of preferences » was suggested for the studied mixtures:

[GAP/HNIW] < [(AMMO-BAMO)/HMX] < [GAP/HMX] < [(AMMO-BAMO)/HNIW]

On the left side stands the minimal response and on the right side – the maximal one.
The « sequence of preferences » is the base for estimations of 'combustion quality' of new mixture burning in field of pulsating pressure.
The « sequence of preferences » obtained by the linear approach, probable, will be valid also for nonlinear cases.

Recommendations

In future work must be investigated combustion mechanisms of mixtures on base of HNIW, with catalytic additions, correcting burning rates, and having new binders. It is important to perform investigations of gas velocity driven burn-rate response functions.

TABLES OF FINAL REPORT (item 0001AD)

Table 1: Burning wave parameters of mixture 1 (GAP/HNIW, 20:80, 1.77 g/cm^3) at pressure p and sample temperature T_o variations. Presented at T_o,°C: -100/20/100.

N	p, MPa	0.1	0.5	1.0	2.0	5.0	8.0	10.0
1	m, g/cm^{2}s	-/0.28 /0.35	0.37/0.5 /65	0.58/0.8 /0.95	0.95/1.25 /1.4	1.8/2.05 /2.3	2.65/3.25 /3.65	3.3/4 /~4.45
2	T_s, °C	-/248 /255	256/270 /278	270/285 /292	290/303 /308	315/324 /328	330/344 /350	345/355 /360
3	$\varphi \cdot 10^{-4}$, K/cm	-/2/2	3.3/3/3	4.5/4/3.5	6.5/5.5/4.5	10/9/7.5	12.6/11/10	14/13/12
4	q, cal/g	-/12 /9.7	15.6/10.5 /8.3	13.6/9 /6.6	12.3/8 /6	10.6/8 /6.2	9/6.6 /5.4	8.3/6.3 /5.4
5	q_r, cal/g	-/7/5.7	5.4/4/3	2.5/2.5/2	2.1/4/3.6	7.8/6.8/6	9/7.4/6.6	7.3/8/7.2
6	Q, cal/g	-/61/39	104/73/51	114/81/59	122/87/63	127/91/68	133/99/76	140/103/78
7	l, μm	-/87/75	80/70/55	65/55/45	48/45/40	35/33/30	30/27/20	25/23/20
8	l_m, μm	-/50/60	40/40/40	30/30/36	20/25/32	15/20/28	12/17/20	10/15/18
9	$\chi \cdot 10^3$, cm^2/s	- /1.4/1.5	1.7/2.0 /2.0	/2.1/2.5 /2.5	2.6/3.0 /3.2	3.6/4.0 /4.0	4.2/5.0 /4.5	4.6/5.5 /5.0
10	$\lambda_s \cdot 10^4$, cal/cm·s·K	- /8.7/9.3	10/12 /12.5	13/16.7 /15.5	16/18.6 /20	23/24 /25	26/31 /28	28/34 /31
11	T_l, °C	-/800 /850	880/900 /950	980/1000 /1150	1150/ /1250	-/-/1350	-/-/-	-/-/-
12	T_f, °C	-/-/-	-/2500 /2550	2500/2600 /2650	2630/2750 /2800	2750/2850 /2950	2850/2930 /3000	2850/2930 3000/
13	L_1, mm	-/>3/>5	>5/2/1.5	2.5/1.5/1.3	0.9/1.0/1.2	-/-/0.3	-/-/-	-/-/-
14	L, mm	-/-/-	-/4/2.5	5/4/3	3.5/3/4	2.8/2.5/3.5	1.8/2.0/3	1.6/1.8/2
15	ϑ, μm	-/28 /23	22/18 /13	15/11 /10	10/7.8 /7.0	6.0/5.2 /5.0	4.0/3.3 /3.0	3.2/2.7 /2.5
16	Ω	-/107 />220	>220/111 /110	160/136 /127	90/128 /167	475/240 /43	450/303 /500	500/333 /750
17	W_o, kcal/cm^{3}s	-/1.9 /2.3	4.0/5.0 /6.6	8.7/11 /11.2	20.7/23 /21.4	60/63 /58.7	113/122 /125	156/177 /183

Table 2: Burning wave parameters of mixture 2 ({BAMO-AMMO}/HNIW, 20:80, 1.76 g/cm^3) at pressure p and sample temperature T_o variations. Presented at T_o,°C: -100/-50 /20/100.

N	p, MPa	0.5	1.0	2.0	5.0	8.0	10.0
1	m, g/cm^{2}s	-/0.7 /0.8/1.1	0.75/1.0 /1.2/1.55	1.15/1.55 /2.1/2.5	2.4/3.3 /4.4/5.0	3.6/4.6 /6.0/6.9	4.3/5.55 /6.9/~8
2	T_s, °C	-/278 /285/298	280/290 /302/312	296/308 /325/332	326/340 /360/365	344/356 /375/382	352/365 /382/~390
3	$\varphi \cdot 10^{-4}$, K/cm	-/4.4 /4/2.8	5.6/5 /4.6/3.5	7/6.5 /6/4.6	11/10.5 /10/8	14.5/13.7 /13/12	16.5/15.8 /15/14
4	q, cal/g	-/11 /9/4.6	13/9 /7/4.2	11/7.8 /5.4/3.5	8.7/6 /4.4/3.1	7.8/5.8 /4.3/3.5	7.7/5.7 /4.3/3.6
5	q_r, cal/g	-/3 /2.5/1.8	2.7/2 /1.6/1.3	4/3.2 /2.4/2	5.8/4.2 /3.5/2.8	6.7/5.2 /4/3.5	6.5/5 /4.6/4
6	Q, cal/g	-/101 /81/63	117/108 /90/69	124/114 /99/76	135/126 /114/87	141/131 /116/92	144/135 /118/94
7	l, μm	-/50 /45/48	50/44 /40/40	40/36 /34/35	30/26 /25/24	22/21 /22/16	20/19 /20/17
8	l_m, μm	-/25 /35/45	15/22 /30/33	13/19 /24/30	10/14 /22/20	8/12 /18/18	12/10 /16/18
9	$\chi \cdot 10^3$, cm^2/s	-/1.7 /2/3	2.1/2.5 /2.7/3.5	2.6/3 /4/5	4/4.8 /5/5.5	5/5.5 /6/6	5.6/6 /6.5/7
10	$\lambda_s \cdot 10^4$, cal/cm·s·K	-/10 /12/16	12/15 /16/20	16/19 /22/28	25/29 /32/35	28/33 /35/40	30/35 /40/43
11	T_l, °C	-/900 /1000/1100	850/950 /1050/1150	900/1000 /1100/1180	950/1050 /1150/1200	-/- /-/-	-/- /-/-
12	T_f, °C	-/2140 /2200/2250	2200/2300 /2400/2500	2500/2540 /2600/2700	2700/2770 /2850/2950	2800/2850 /2930/3000	2800/2850 /2930/3000
13	L_1, mm	-/0.8 /1.0/1.5	0.5/0.7 /0.9/1.2	0.5/0.6 /0.6/0.7	0.2/0.3 /0.25/0.4	-/- /-/-	-/- /-/-
14	L, mm	-/3.5 /5.0/5.0	2.5/3.5 /5.0/6.0	2/3.1 /4.5/5.0	1.8/2.8 /4.0/4.5	1.5/2.1 /3.0/3.5	1.4/1.7 /2.0/2.5
15	ϑ, μm	-/12 /12/9.4	11/9 /8.4/6.9	7.4/6 /4.9/4.4	3.7/2.8 /2.4/2.2	3/2.4 /2.1/1.9	2.5/2 /1.8/1.6
16	Ω	-/67 /83/160	45/78 /110/170	68/100 /122/160	54/110 /100/180	500/875 /1430/790	560/850 /1100/940
17	W_o, kcal/cm^{3}s	-/10 /11/10	14/17 /19/18	27/34 /43/39	89/117 /150/138	177/214 /270/280	240/300 360/380

Table 3: Burning wave parameters of mixture 3 (GAP/HMX, 20:80, 1.74 g/cm^3) at pressure p and sample temperature T_o variations. Presented at T_o: -100°C/20°C/90°C

N	p, MPa	0.5	1.0	2.0	5.0	10.0
1	m, g/cm^{2}s	-/0.1/-	0.155/0.21/0.26	0.28/0.37/0.43	0.64/0.77/0.88	1.1/1.26/-
2	T_s, °C	-/330/-	345/365/375	380/400/410	445/460/470	485/492/-
3	$\varphi \cdot 10^{-4}$, K/cm	-/3.5/-	2.0/4.0/5.0	3.5/5.0/7.8	9.0/10/11	11.5/12/-
4	q, cal/g	-/64/-	35/37/42	29/31/43	35/30/33	27/25/-
5	q_r, cal/g	-/0.7/-	0.8/0.7/0.6	0.8/.06/0.6	2.7/2.6/2.4	3.7/3.7/-
6	Q, cal/g	-/78/-	152/120/90	180/140/103	215/164/140	223/180/-
7	l, μm	-/168/-	150/108/106	108/78/75	50/58/54	48/48/-
8	l_m, μm	-/45/-	30/40/55	30/35/40	40/30/38	20/20/-
9	$\chi \cdot 10^3$, cm^2/s	-/1.0/-	1.0/1.3/1.6	1.7/1.7/1.9	2.3/2.5/2.8	3.1/3.3/-
10	$\lambda_s \cdot 10^4$, cal/cm·s·K	-/6.7/-	6.7/9.0/11	12/12/13	16/17/19	22/23/-
11	T_l, °C	-/980/-	-/1050/1000	-/-/1100	-/-/-	-/-/-
12	T_f, °C	-/1900/-	1950/2050 /2150	2150/2200 /2280	2300/2420 /2500	2300/2420/-
13	L_1, mm	-/600/-	-/500/900	-/-/350	-/-/-	-/-/-
14	L, mm	-/2.0/-	1.5/1.7/2.3	1.5/1.6/2.3	2.0/2.0/2.5	1.5/1.7/-
15	ϑ, μm	-/43/-	43/24/19	20/15/13	21/8.0/7.0	5.6/4.9/-
16	Ω	-/15/-	35/96/120	75/106/180	95/250/360	270/300/-
17	W_o, kcal/cm^{3}s	-/1.4/-	1.3/3.5/5.5	4.1/7.8/14	24/33/40	54/64/-

Table 4: Burning wave parameters of mixture 4 ({BAMO-AMMO}/HMX, 20:80, 1.72 g/cm^3) at pressure p and sample temperature T_o variations. Presented at T_o: -100°C/20°C/90°C

N	p, MPa	0.5	1.0	2.0	5.0	10.0
1	m, g/cm^{2}s	-/0.1/-	0.16/0.220.28	0.32/0.41/0.48	0.72/0.85/0.98	1.24/1.44/-
2	T_s, °C	-/330/-	345/365/380	390/407/420	460/470/480	492/500/-
3	$\varphi \cdot 10^{-4}$, K/cm	-/2.2/-	3.4/3.7/5.0	5.0/6.0/6.5	8.0/9.0/11.0	10.4/12.0/-
4	q, cal/g	-/46/-	44.6/37.0/41.0	36.0/34.0/33.0	27.0/26.0/29.0	22.0/22.0/-
5	q_r, cal/g	-/0.6/-	.06/0.6/0.4	.05/0.4/0.4	2.0/1.8/1.7	3.4/4.0/-
6	Q, cal/g	-/96/-	150/120/93	180/140/120	215/172/145	230/185/-
7	l, μm	-/195/-	142/110/100	100/80/78	45/58/55	53/45/-
8	l_m, μm	-/35/-	35/34/40	30/35/40	25/30/45	20/30/-
9	$\chi \cdot 10^3$, cm^2/s	-/1.1/-	1.2/1.4/1.6	1.7/1.9/2.1	2.7/2.8/3.1	3.6/3.8/-
10	$\lambda_s \cdot 10^4$, cal/cm·s·K	-/7.6/-	8.3/9.6/11.0	11.7/13/14	18.5/19.3/21	24.8/26/-
11	T_l, °C	-/900/-	-/1020/1050	-/-/-	-/-/-	-/-/-
12	T_f, °C	-/1850 /-	2000/2100 2200	2200/2300 /2350	2280/2380 /2450	2300/2400 /-
13	L_1, mm	-/500/-	-/400/700	-/-/-	-/-/-	-/-/-
14	L, mm	-/2.2/-	1.9/2.0/2.3	2.0/2.2/2.3	1.7/2.0/2.2	1.1/1.0/-
15	ϑ, μm	-/51/-	32/24/20	17/13/12	8.3/7.0/6.2	4.9/4.0/-
16	Ω	-/9.8/-	53/17/35	100/154/167/	145/258/323/	204/225/-
17	W_o, kcal/cm^{3}s	-/0.9/-	2.2/3.4/6.0	6.7/10/13	24/33/46	55/73/-

Table 5: Coefficients of heat conduction λ_g and specific heat c_p of the gas phase

mixtures	T, °C	300	500	800	1000	1500
GAP/HNIW	$\lambda_g \cdot 10^4$, cal/cm·c·K	1.6	2.1	2.8	3.3	4.4
	c_p, cal/g·K	0.33	0.34	0.36	0.37	0.40
(BAMO-AMMO)/HNIW	$\lambda_g \cdot 10^4$, cal/cm·c·K	1.6	2.1	2.8	3.4	4.5
	c_p, cal/g·K	0.33	0.34	0.36	0.37	0.40
GAP/HMX	$\lambda_g \cdot 10^4$, cal/cm·c·K	2.0	2.6	3.4	4.0	5.6
	c_p, cal/g·K	0.41	0.43	0.45	0.46	0.50
(BAMO-AMMO)/HMX	$\lambda_g \cdot 10^4$, cal/cm·c·K	1.9	2.5	3.3	3.9	5.5
	c_p, cal/g·K	0.41	0.43	0.45	0.46	0.50

Table 6: Sensitivities of burning rate and surface temperature to pressure and sample temperature of the studied mixtures. Sample temperature T_o=20°C

Systems	P, MPa	0.1	0.5	1	2	5	8	10	Activation energy of gasification
	property								
Mixture 1	β,%/K	0.28	0.31	0.23	0.19	0.13	0.17	0.15	E, Kcal/mol
	k	0.63	0.78	0.60	0.54	0,40	0,55	0,50	
GAP/HNIW,	ν	0.37	0.50	0.60	0.60	0,80	0,93	0,93	
	r	0.088	0.106	0.102	0.08	0,06	0,09	0,075	**32.8**
	μ	0.06	0.076	0.09	0.084	0,08	0,14	0,136	
	T_s, K	521	543	558	576	597	617	628	
	β,%/K	-	0.28	0.30	0.36	0.30	0.30	0.28	
Mixture 2	k	-	0.74	0.85	1.10	1.02	1.12	1.01	
	ν	-	0.55	0.70	0.82	0.73	0.68	0.68	
(AMMO-	r	-	0.13	0.15	0.15	0.18	0.18	0.20	**32.8**
BAMO)/HNIW,	μ	-	0.10	0.12	0.115	0.11	0.10	0.10	
	T_s, K	-	558	575	598	633	648	655	
Mixture 3	β,%/K	-	-	0.28	0.23	0.18	0.17	0.17	
	k	-	-	0,97	0,87	0,79	0,787	0,80	
GAP/HMX,	ν	-	-	0,83	0,80	0,76	0,76	0,76	
	r	-	-	0,17	0,155	0,13	0,10	0,09	**28.0**
	μ	-	-	0,16	0,165	0,115	0,104	0,092	
	T_s, K	-	-	638	673	733	756	765	
Mixture 4	β,%/K	-	-	0.28	0.20	0.16	0.13	0.12	
	k	-	-	0,95	0,759	0,72	0,61	0,576	
(AMMO-	ν	-	-	0,90	0,82	0,80	0,79	0,79	
BAMO)/HMX,	r	-	-	0,19	0,16	0,105	0,066	0,067	**28.0**
20:80	μ	-	-	0,174	0,168	0,11	0,094	0,092	
	T_s, K	-	-	638	680	743	763	773	

Table 7: Dependencies of sensitivities for burning rate and surface temperature of system (AMMO-BAMO)/HNIW, 20:80, at negative sample temperatures. Criteria of stable combustion.

p, MPa	0.5		1		2		5		8		10	
T_o,°C	-100	-50	-100	-50	-100	-50	-100	-50	-100	-50	-100	-50
β,%/K	-	0.20	0.56	0.44	0.47	0.47	0.42	0.42	0.42	0.42	0.40	0.40
k	-	0.66	2.13	1.5	1.87	1.68	1.80	1.64	1.80	1.70	1.37	1.25
r	-	0.10	0.20	0.19	0.20	0.23	0.22	0.25	0.24	0.25	0.27	0.25
k*	-	-	**2.0**	0.5	**1.32**	0.7	**1.03**	0.55	0.93	0.5	0.2	0.1

Table 8: Response function characteristics of the studied mixtures. Linear approximation, T_o=20°C.

		Properties									
Systems	**p, MPa**	**Re{U}$_m$**	**ω_n**	**ϖ_n, KHz**	**Re{U}$_{20}$**	**Im {U} max+**	**ω_{im+}**	**ϖ_{im+}, KHz**	**Im {U} min**	**ω_{im-}**	**ϖ_{im-}, KHz**
GAP/ HNIW	**0.1**	0.55	6.75	0.12	0.46	0.07	1.0	0.018	-0.12	15	0.28
	0.5	0.86	5.75	0.23	0.70	0.14	1.25	0.05	-0.24	16	0.63
	1	0.87	5.5	0.45	0.73	0.11	1.0	0.08	-0.17	17	1.38
	2	0.84	6.0	0.98	0.76	0.10	1.0	0.16	-0.14	18	2.93
	5	1.04	7.75	2.56	1.00	0.10	1.0	0.33	-0.08	18	5.94
	8	1.30	6.0	4.02	1.18	0.15	1.0	0.67	-0.24	18	12.1
	10	1.27	6.0	5.52	1.20	0.14	1.0	0.92	-0.20	18	16.6
(AMMO-BAMO)/ HNIW	**0.5**	0.86	4.5	0.45	0.75	0.13	1.0	0.10	-0.26	17	1.72
	1	1.21	4.75	0.81	0.80	0.21	1.25	0.21	-0.39	18	3.1
	2	2.03	6.0	2.12	1.20	0.49	1.75	0.62	-0.80	17	6.0
	5	1.51	4.75	5.9	0.80	0.32	1.5	1.88	-0.52	15	18.8
	8	1.62	5.0	9.7	0.80	0.39	1.75	3.4	-0.60	14	27
	10	1.36	4.5	10.6	0.80	0.29	1.25	2.95	-0.40	13	30
GAP/ HMX	**1**	1.56	4.5	0.05	0.90	0.29	1.25	0.014	-0.60	15	0.17
	2	1.36	4.5	0.12	0.85	0.22	1.0	0.026	-0.50	15	0.39
	5	1.28	5.25	0.40	0.90	0.22	1.25	0.096	-0.36	16	1.23
	8	1.34	6.5	0.83	0.93	0.23	1.5	0.19	-0.34	16	2.1
	10	1.40	7.5	1.18	1.20	0.26	1.5	0.24	-0.32	18	2.8
(AMMO-BAMO)/ HMX	**1**	1.62	4.0	0.05	0.95	0.29	1.0	0.014	-0.59	15	0.20
	2	1.26	4.0	0.12	0.95	0.18	1.0	0.03	-0.40	15	0.45
	5	1.31	6.0	0.52	0.80	0.21	1.25	0.11	-0.30	18	1.55
	8	1.22	8.0	1.18	0.79	0.17	1.25	0.19	-0.18	18	2.66
	10	1.18	7.75	1.44	0.79	0.16	1.0	0.19	-0.16	20	3.72

Table 9. Response function characteristics at nonlinear approximations: Second order interaction of the first and second harmonics. Values of $Re\{V_1\}_m/\ \omega_n$ are presented. T_o=20°C.

Parameter n is a coefficient in expression: $p_1=n \cdot p_o$;

	p, MPa	0.1		0.5		1.0		2.0		5.0		10	
	n	0.1	0.3	0.1	0.3	0.1	0.3	0.1	0.3	0.1	0.3	0.1	0.3
Systems	ψ												
GAP/ HNIW	0	0.53 /8.0	0.70 /20	0.87 /11	1.1/ 20	0.85 /11	1.0 /20	0.81 /14	0.90 /20	1.0 /20	0.96 /20	1.23 /20	1.40 /20
	$\pi/2$	0.51 /4.0	0.46 /1.0	0.73 /3.0	0.66 /2.0	0.78 /3.0	0.73 /1.0	0.77 /3.0	0.72 /1.0	0.96 /3.0	0.93 /1.0	1.1 /2.0	1.1 /1.0
	π	-	-	0.90 /4.0	-	0.94 /4.0	1.1 /2.0	0.90 /5	-	1.15 /5.0	1.38 /4.0	1.4 /5.0	1.8 /3.0
	$3\pi/2$	-	-	1.0 /8.0	-	1.0 /8.0	1.3 /10	0.97 /10	-	1.22 /20	1.64 /20	1.55 /12	2.2 /18
(AMMO-BAMO)/ HNIW	0	-	-	0.86 /8.0	1.1 /15	1.3 /9.0	1.76 /16	2.9 /10	5.1 /11	1.8 /8.0	2.7 /10	1.55 /8.0	2.2 /10
	$\pi/2$	-	-	0.70 /3.0	0.70 /1.0	0.98 /2.0	0.92 /1.0	1.33 /2.0	1.34 /1.0	1.1 /2.0	1.0 /1.0	1.0 /2.0	0.94 /1.0
	π	-	-	0.92 /3.0	-	1.32 /3.0	1.63 /3.0	2.4 /4.0	-	1.7 /3.0	2.1 /3.0	1.46 /3.0	1.83 /2.0
	$3\pi/2$	-	-	1.0 /6.0	-	1.54 /6.0	2.23 /6.0	3.4 /6.0	-	2.1 /5.0	3.3 /5.0	1.82 /5.0	2.75 /5.0
GAP/ HMX	0	-	-	-	-	1.8 /8.0	2.8 /10	1.5 /8.0	2.14 /12	1.36 /12	1.9 /19	1.55 /17	2.3 /20
	$\pi/2$	-	-	-	-	1.16 /2.0	1.13 /1.0	1.1 /2.0	1.0 /1.0	1.05 /2.0	1.0 /1.0	1.1 /3.0	1.1 /1.0
	π	-	-	-	-	1.77 /3.0	-	1.5 /3.0	1.9 /2.0	1.42 /4.0	-	1.5 /5.0	2.1 /4.0
	$3\pi/2$	-	-	-	-	2.23 /5.0	-	1.8 /5.0	2.7 /6.0	1.65 /7.0	-	1.9 /10	3.0 /11
(AMMO-BAMO)/ HMX	0	-	-	-	-	1.87 /8.0	2.87 /10	1.3 /9.0	1.74 /13	1.36 /16	1.9 /20	1.16 /20	1.3 /20
	$\pi/2$	-	-	-	-	1.2 /2.0	1.17 /1.0	1.0 /2.0	0.95 /1.0	1.1 /2.0	1.05 /1.0	1.0 /3.0	1.0 /1.0
	π	-	-	-	-	1.8 /3.0	-	1.4 /3.0	1.7 /2.0	1.46 /4.0	-	1.32 /5.0	1.64 /5.0
	$3\pi/2$	-	-	-	-	2.23 /5.0	-	1.6 /5.0	2.22 /6.0	1.67 /8.0	-	1.46 /14	2.14 /20

Table 10. Response function characteristics at nonlinear approximations: Second order self-interaction of the first harmonic. Values of $Re\{V_2\}_m / \omega_n$ are presented. T_o=20°C.

Parameter n is a coefficient in expression: $p_1=n \cdot p_o$;

Systems	p, MPa	0.1		0.5		1.0		2.0		5.0		10	
	n	0.1	0.6	0.1	0.6	0.1	0.6	0.1	0.6	0.1	0.6	0.1	0.6
GAP/ HNIW	ψ												
	0	0.51 /2.0	0.53 /2.0	0.86 /3.0	0.90/ 3.5	0.88 /3	0.95 /3.25	0.86 /3.5	0.92 /3.5	1.1 /4.0	1.17 /5.0	1.9 /3.75	1.44 /4.0
	$\pi/2$	0.51 /2.0	0.52 /2.0	0.86 /3.0	0.89 /3.25	0.88 /2.75	0.90 /3.0	0.85 /3.0	0.87 /3.25	1.1 /4.0	1.1 /3.75	1.27 /3.0	1.32 /3.0
	π	-	-	0.85 /2.75	-	0.86 /2.5	-	0.83 /3.0	-	1.02 /4.0	-	1.24 /2.75	-
	$3\pi/2$	-	-	0.85 /3.0	-	0.86 /2.5	-	0.84 /3.0	-	1.04 /4.0	-	1.26 /3.0	-
(AMMO-BAMO)/ HNIW	0	-	-	0.87 /2.0	0.92 /3.0	1.21 /2.0	1.3 /2.5	2.0 /3.0	2.0 /3; 9	1.52 /2.5	1.57 /2.74	1.38 /2.25	1.43 /2.75
	$\pi/2$	-	-	0.86 /2.0	0.90 /3.0	1.22 /2.5	1.3 /2.5	2.05 /3.0	2.3 /5.0	1.53 /2.5	1.67 /3.0	1.38 /2.25	1.5 /2.75
	π	-	-	0.85 /2.5	-	1.2 /2.25	-	2.0 /3.0	-	1.5 /2.25	-	1.35 /2.25	-
	$3\pi/2$	-	-	0.85 /2.25	-	1.2 /2.25	-	2.0 /3.0	-	1.48 /2.25	-	1.34 /2.25	-
GAP/ HMX	0	-	-	-	-	1.57 /2.25	1.66 /2.75	1.37 /2.25	1.47 /2.75	1.30 /2.75	1.40 /3.25	1.42 /3.75	1.49 /4.5
	$\pi/2$	-	-	-	-	1.58 /2.25	1.73 /2.75	1.37 /2.25	1.48 /2.5	1.30 /2.75	1.37 /3.0	1.42 /4.0	1.50 /4.0
	π	-	-	-	-	1.54 /2.25	-	1.34 /2.0	-	1.26 /2.5	-	1.40 /3.5	
	$3\pi/2$	-	-	-	-	1.53 /2.25	-	1.34 /2.0	-	1.27 /2.5	-	1.40 /3.75	
(AMMO-BAMO)/ HMX	0	-	-	-	-	1.64 /2.25	1.77 /3.0	1.28 /2.25	1.40 /2.75	1.33 /3.0	1.44 /3.75	1.20 /4.0	1.31 /4.75
	$\pi/2$	-	-	-	-	1.65 /2.0	1.82 /2.5	1.0 /2	1.35 /2.25	1.32 /3.0	1.39 /3.5	1.19 /4.0	1.23 /4.0
	π	-	-	-	-	1.6 /2.25	-	1.4 /3	-	1.28 /3.0	-	1.16 /3.5	-
	$3\pi/2$	-	-	-	-	1.6 /2.0	-	1.6 /5	-	1.29 /3.0	-	1.176 /3.5	-

FIGURES OF FINAL REPORT (item 0001AD)

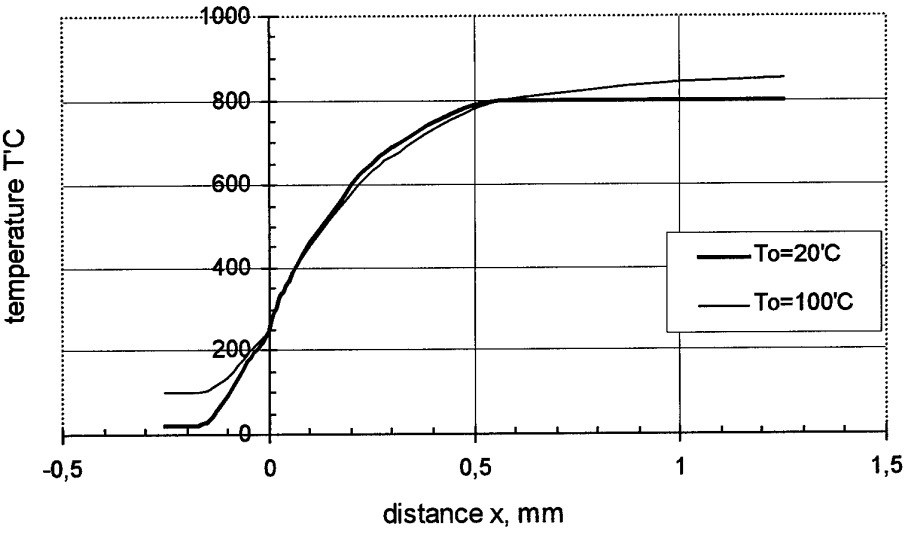

Figure 1: Averaged temperature profiles T(x) of mixture GAP/HNIW, 20/80, at 0.1 MPa and different To.

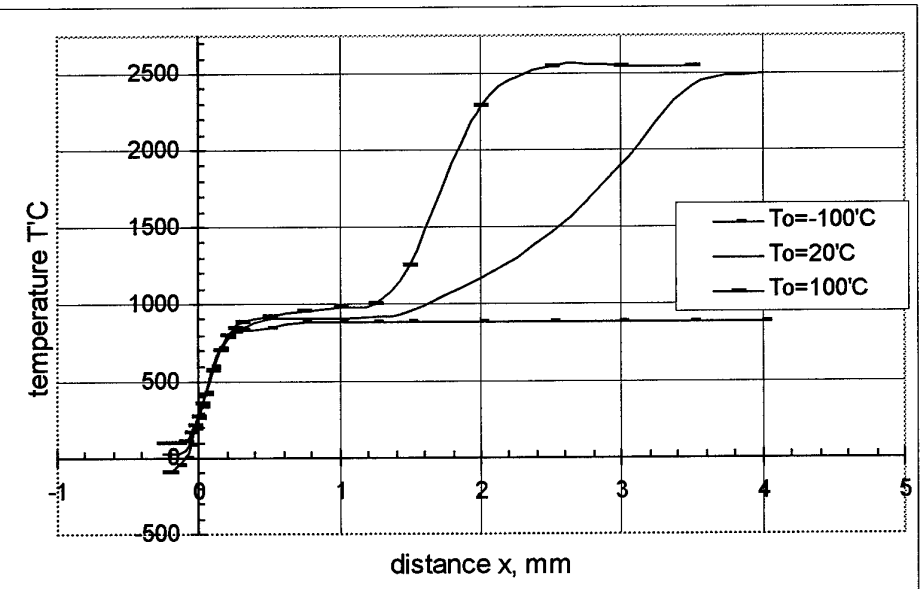

Figure 2: Averaged temperature profiles T(x) of mixture GAP/HNIW, 20/80, at 0.5 MPa and different To.

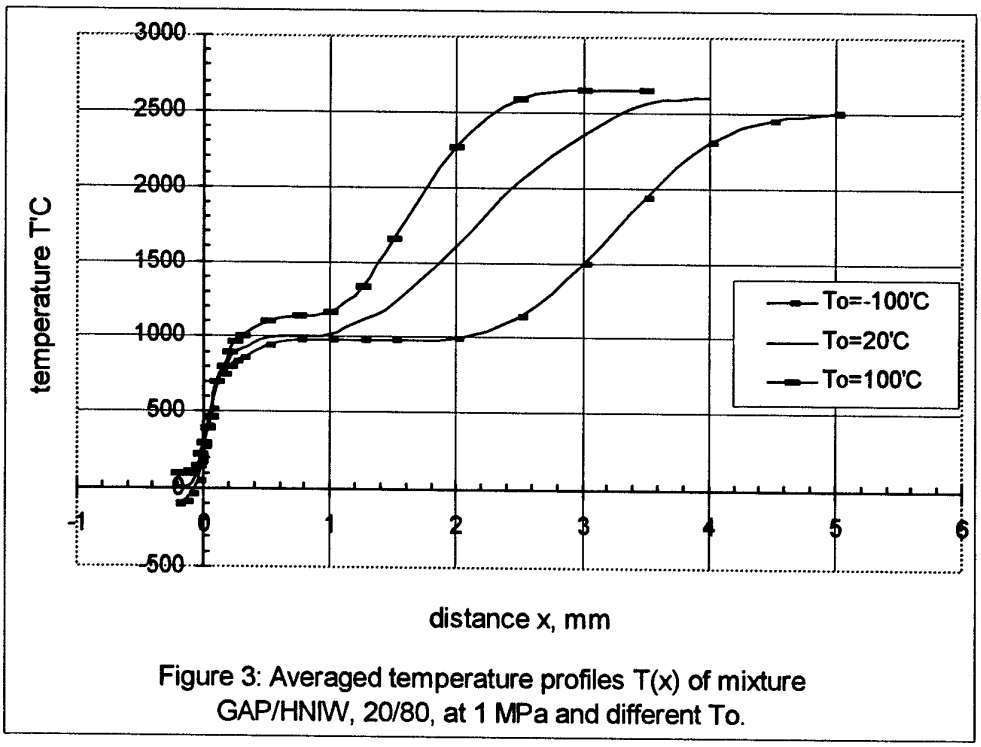

Figure 3: Averaged temperature profiles T(x) of mixture GAP/HNIW, 20/80, at 1 MPa and different To.

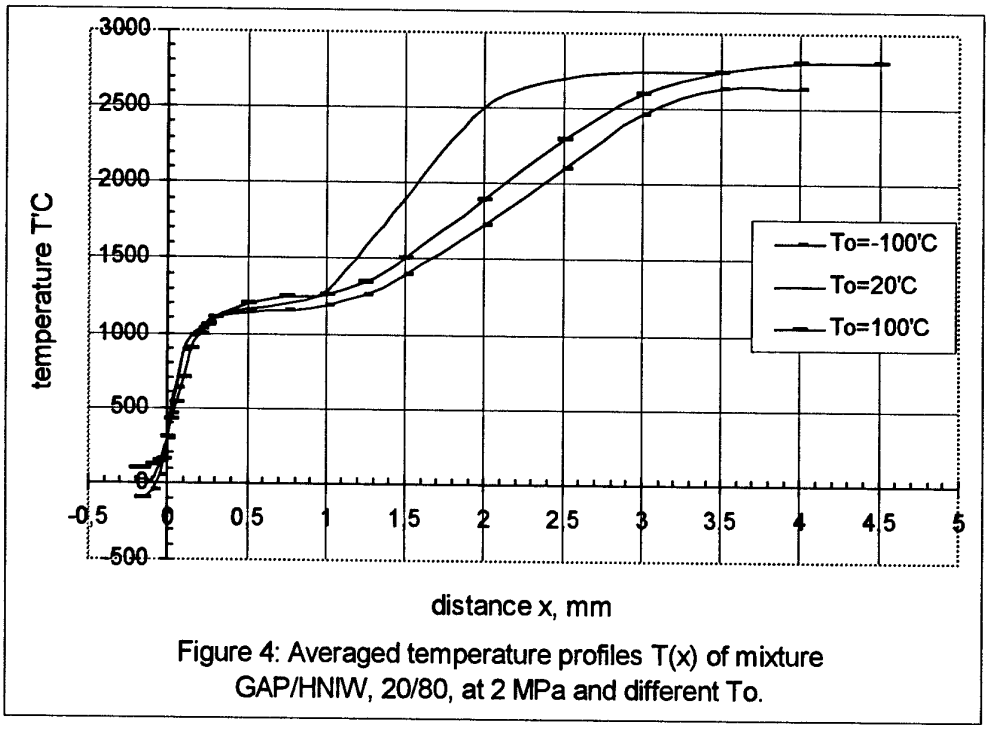

Figure 4: Averaged temperature profiles T(x) of mixture GAP/HNIW, 20/80, at 2 MPa and different To.

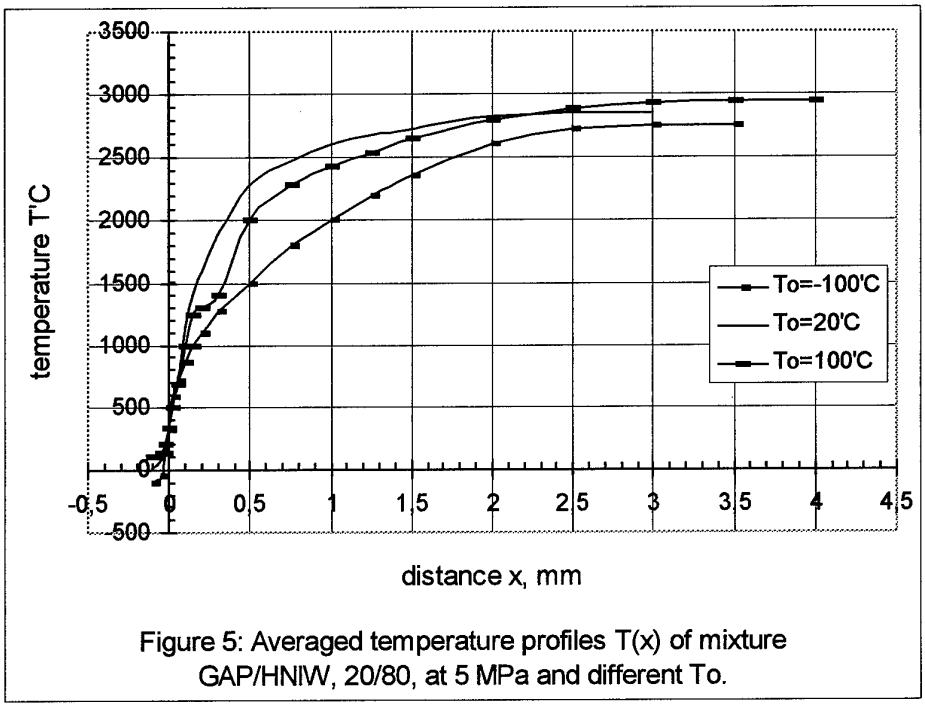

Figure 5: Averaged temperature profiles T(x) of mixture GAP/HNIW, 20/80, at 5 MPa and different To.

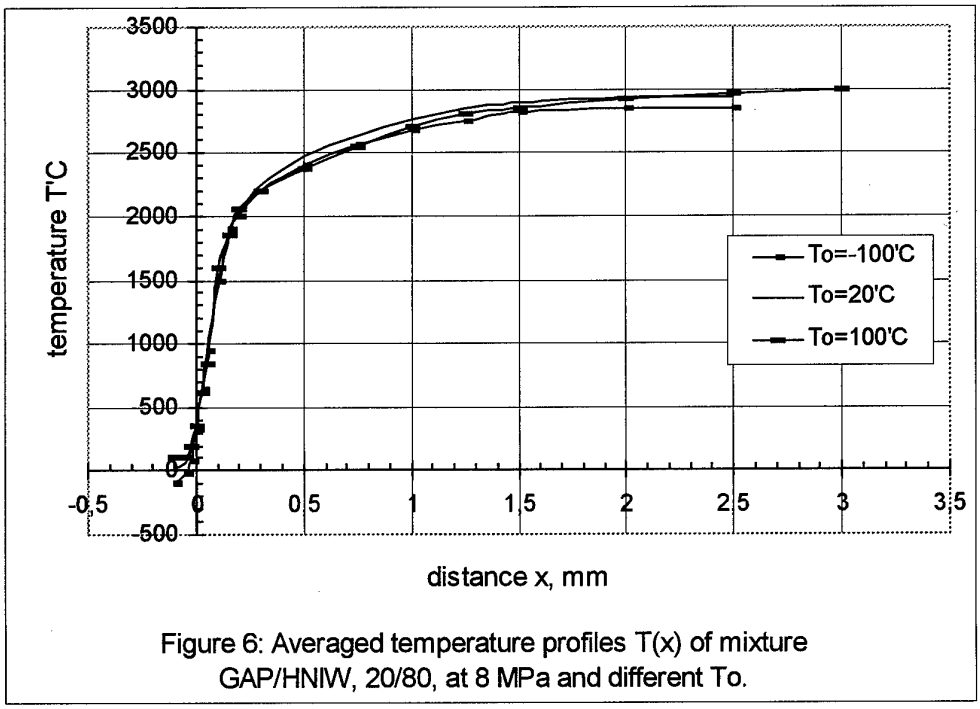

Figure 6: Averaged temperature profiles T(x) of mixture GAP/HNIW, 20/80, at 8 MPa and different To.

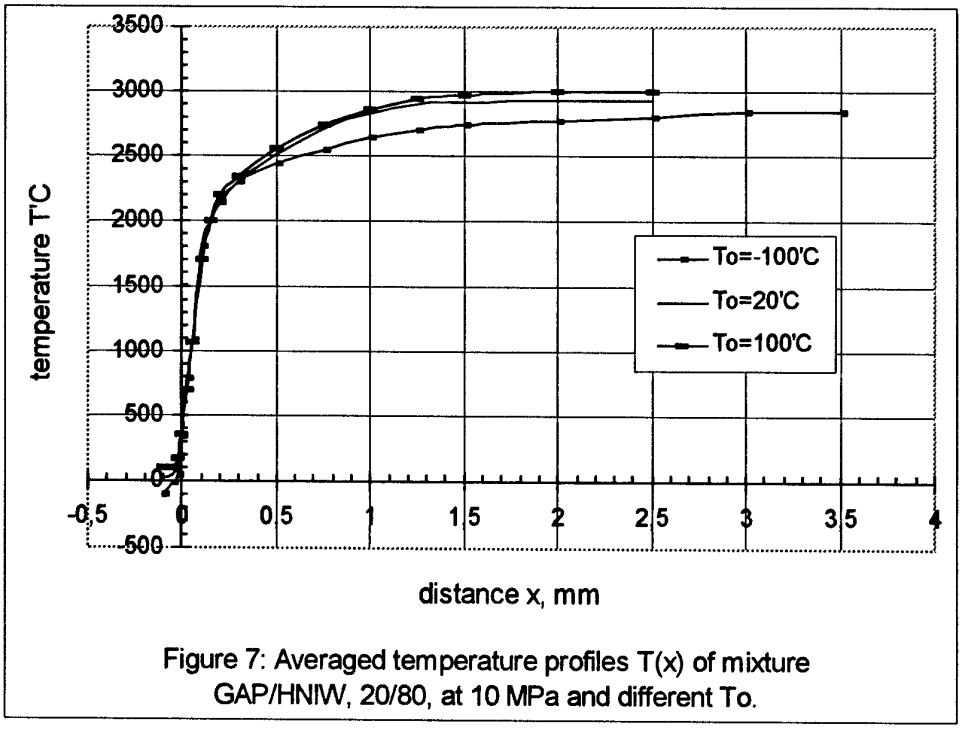

Figure 7: Averaged temperature profiles T(x) of mixture GAP/HNIW, 20/80, at 10 MPa and different To.

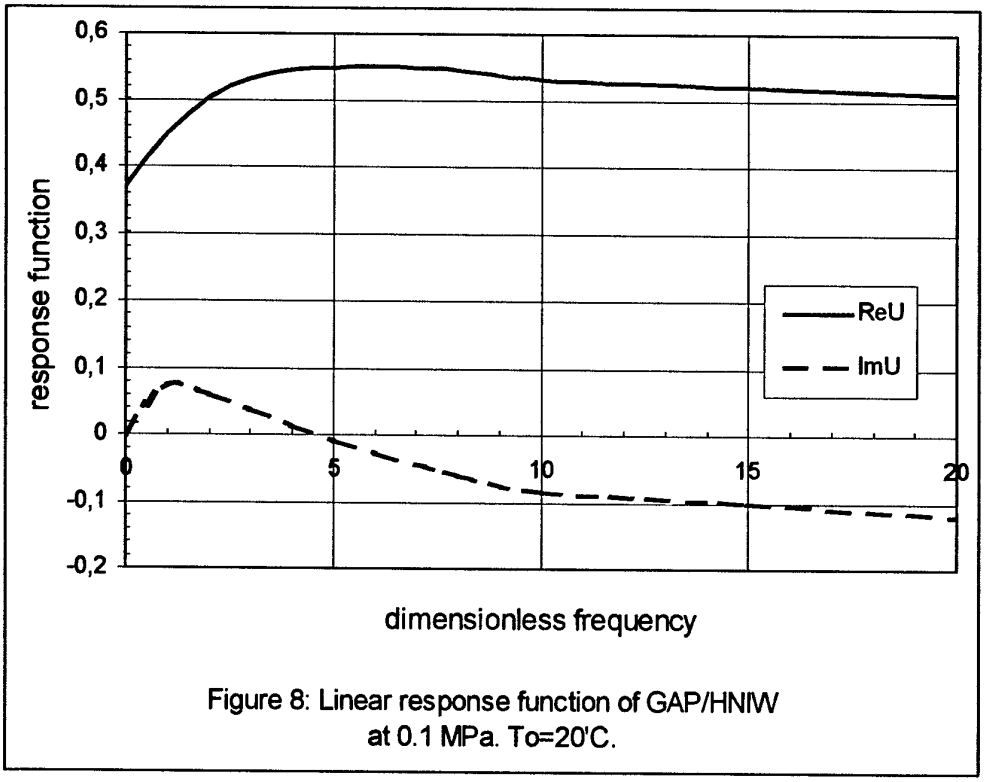

Figure 8: Linear response function of GAP/HNIW at 0.1 MPa. To=20'C.

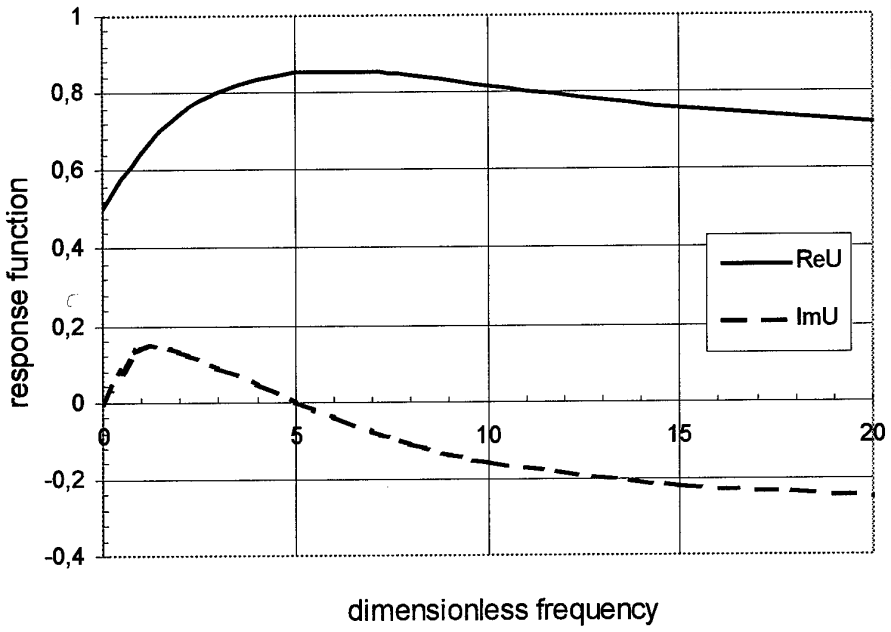

Figure 9: Linear response function of GAP/HNIW
at 0.5 MPa. To=20'C.

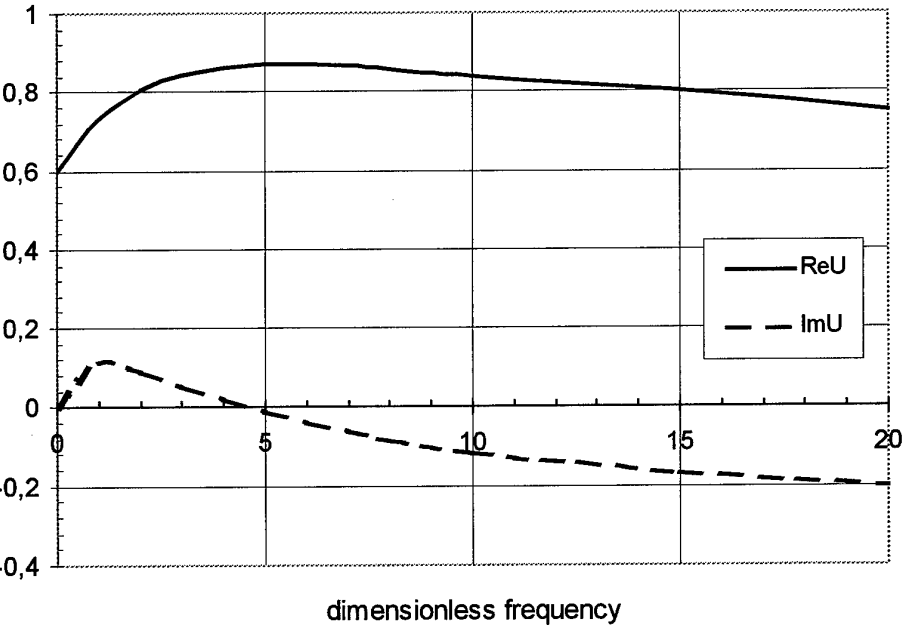

Figure 10: Linear response function of GAP/HNIW
at 1 MPa. To=20'C.

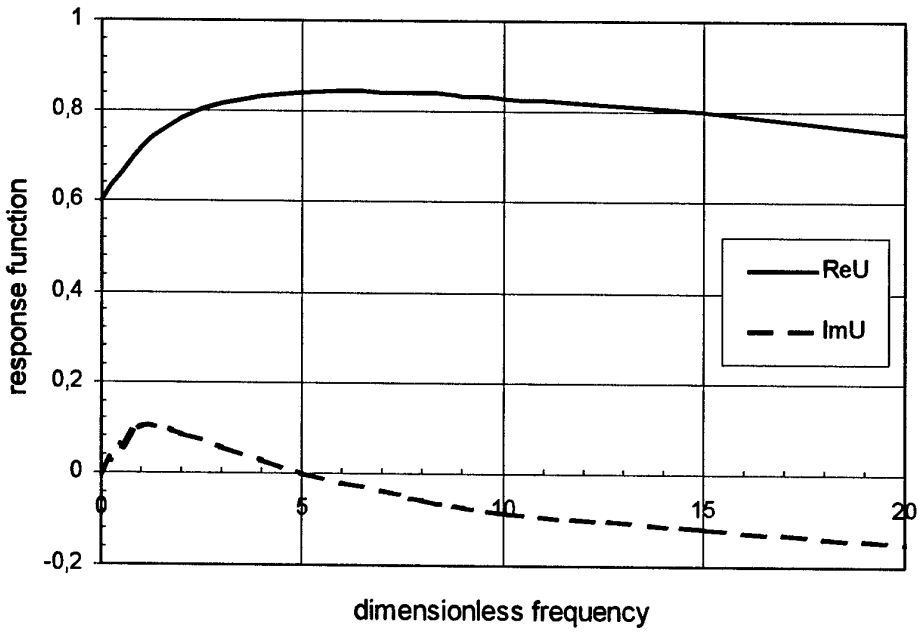

Figure 11: Linear response function of GAP/HNIW at 2 MPa. To=20'C.

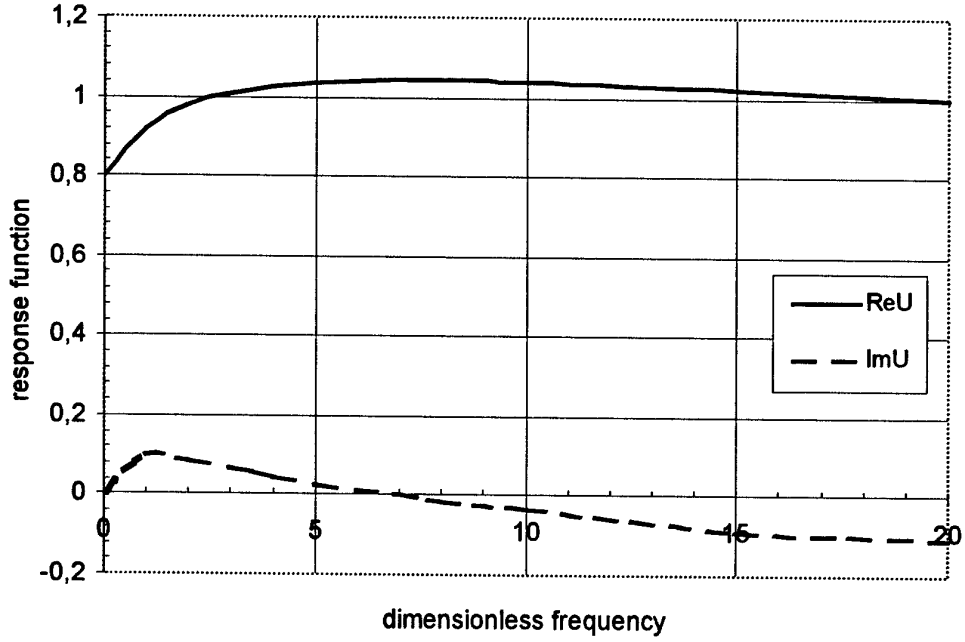

Figure 12: Linear response function of GAP/HNIW at 5 MPa. To=20'C.

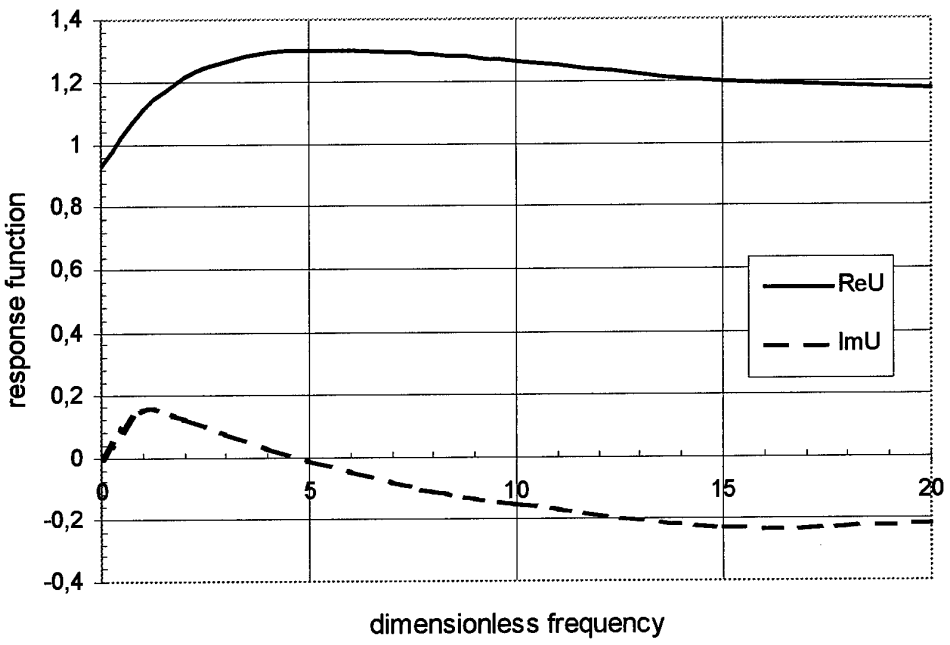

Figure 13: Linear response function of GAP/HNIW
at 8 MPa. To=20'C.

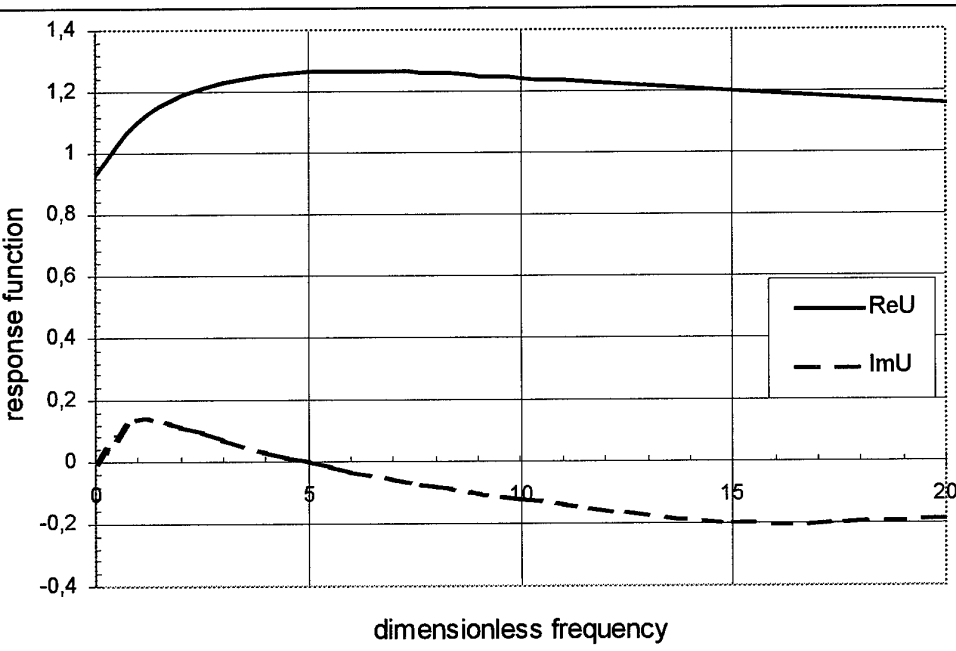

Figure 14: Linear response function of GAP/HNIW
at 10 MPa. To=20'C.

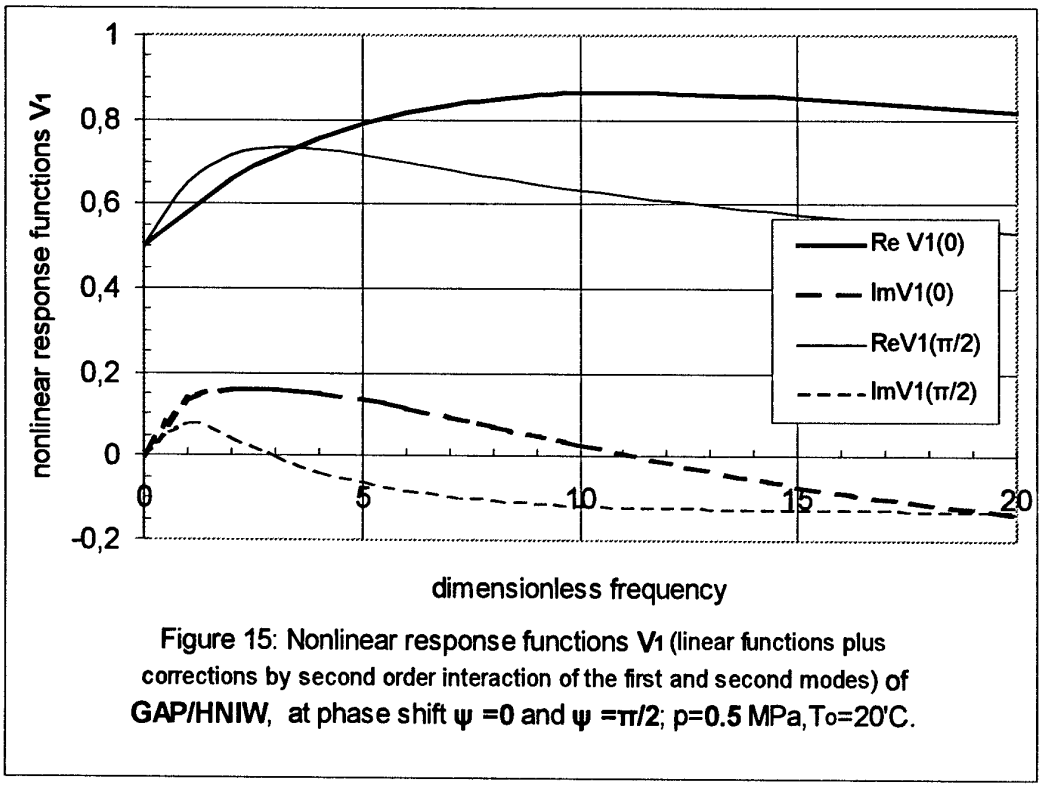

Figure 15: Nonlinear response functions V_1 (linear functions plus corrections by second order interaction of the first and second modes) of **GAP/HNIW**, at phase shift $\psi = 0$ and $\psi = \pi/2$; p=**0.5** MPa, T_o=20'C.

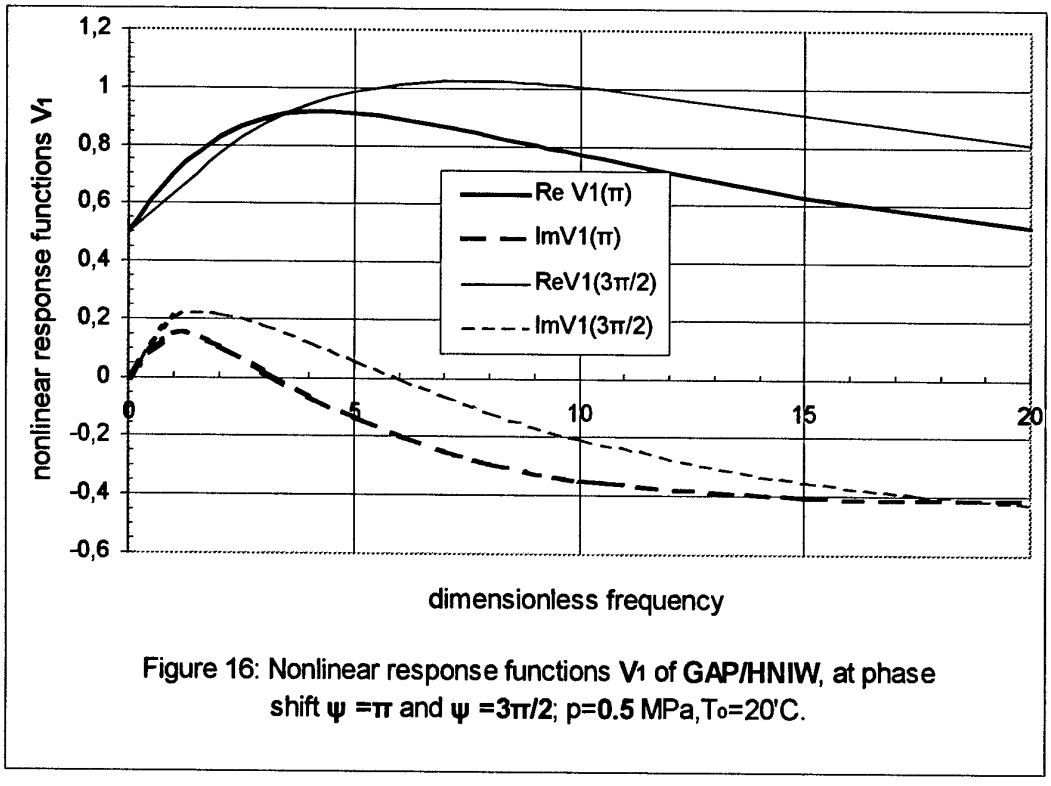

Figure 16: Nonlinear response functions V_1 of **GAP/HNIW**, at phase shift $\psi = \pi$ and $\psi = 3\pi/2$; p=**0.5** MPa, T_o=20'C.

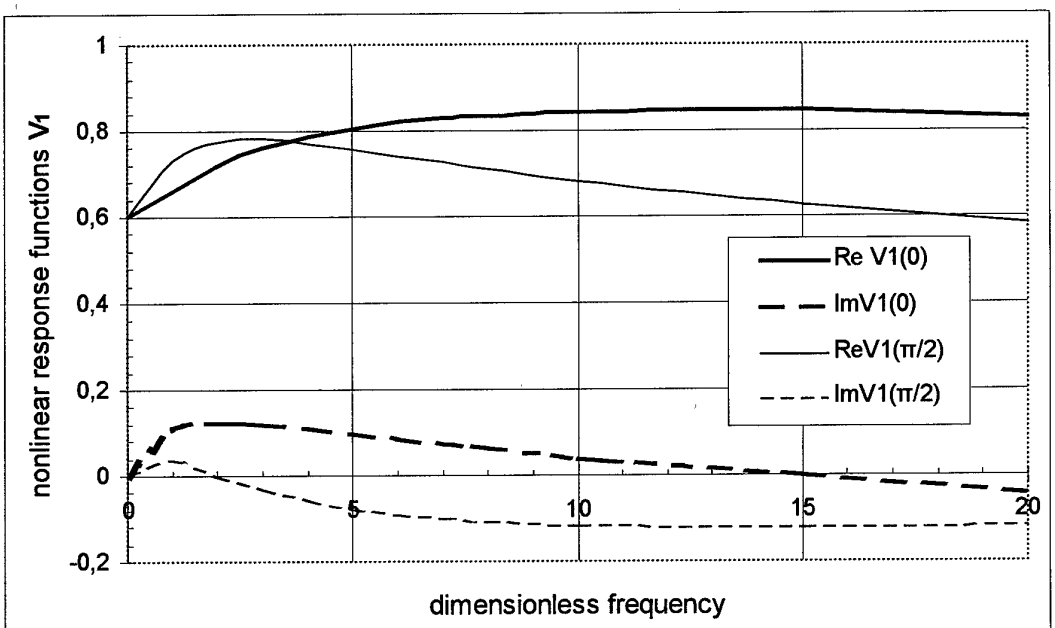

Figure 17: Nonlinear response functions V_1 (linear functions plus corrections by second order interaction of the first and second modes) of **GAP/HNIW**, at phase shift $\psi = 0$ and $\psi = \pi/2$; p=1 MPa, T_o=20'C.

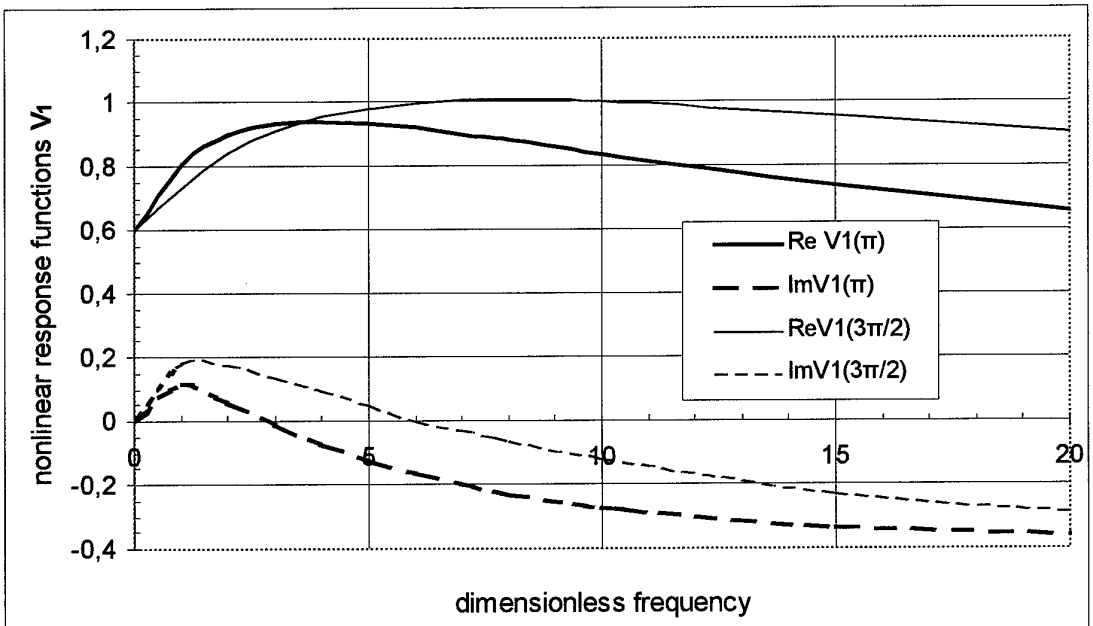

Figure 18: Nonlinear response functions V_1 of **GAP/HNIW**, at phase shift $\psi = \pi$ and $\psi = 3\pi/2$; p=1 MPa, To=20'C

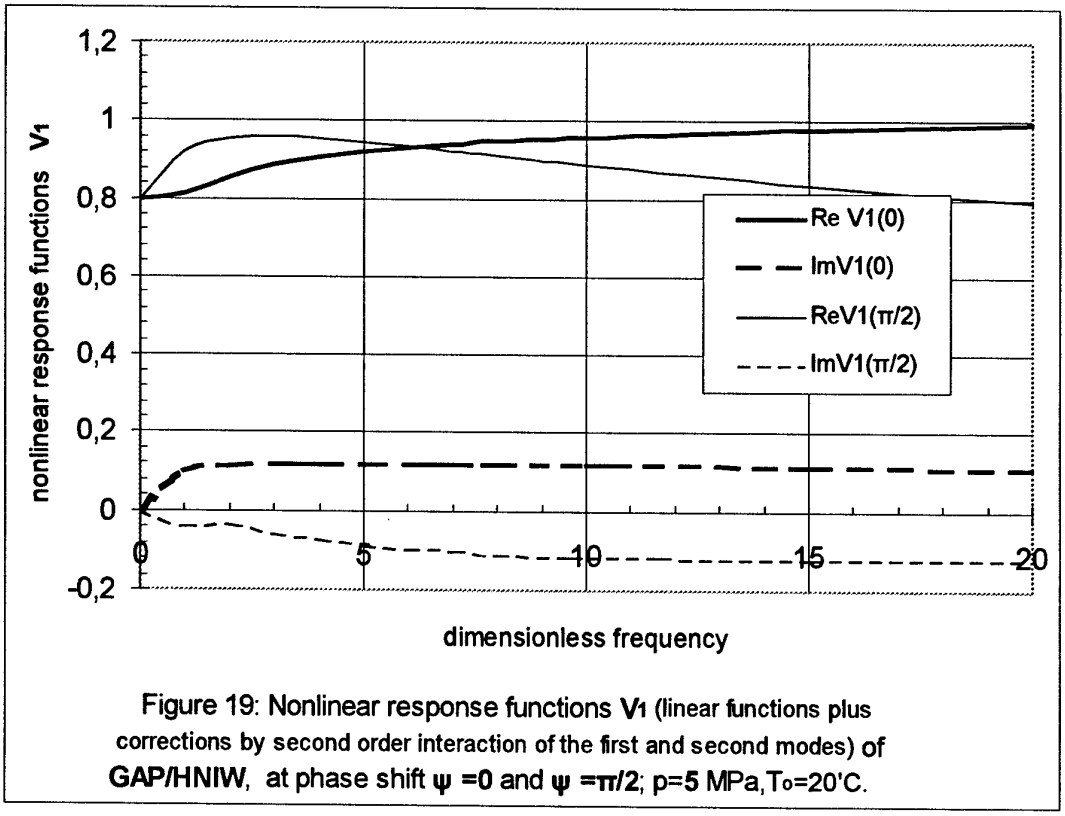

Figure 19: Nonlinear response functions V_1 (linear functions plus corrections by second order interaction of the first and second modes) of GAP/HNIW, at phase shift $\psi = 0$ and $\psi = \pi/2$; p=5 MPa, T_o=20'C.

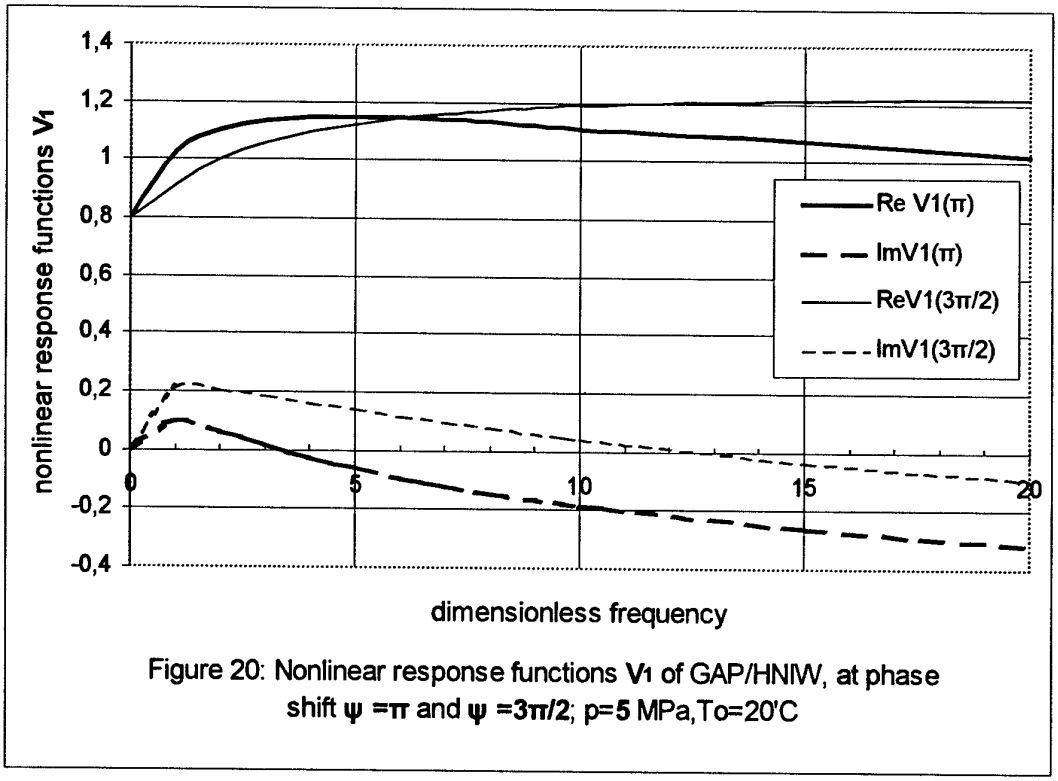

Figure 20: Nonlinear response functions V_1 of GAP/HNIW, at phase shift $\psi = \pi$ and $\psi = 3\pi/2$; p=5 MPa, To=20'C

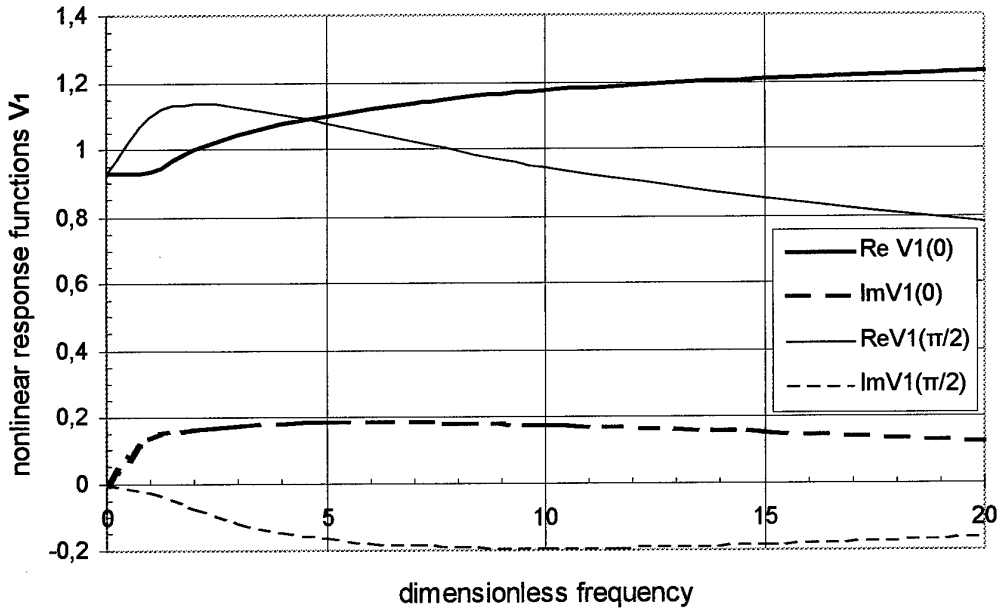

Figure 21: Nonlinear response functions **V1** (linear functions plus corrections by second order interaction of the first and second modes) of **GAP/HNIW,** at phase shift **ψ =0** and **ψ =π/2**; p=**10** MPa,To=20'C.

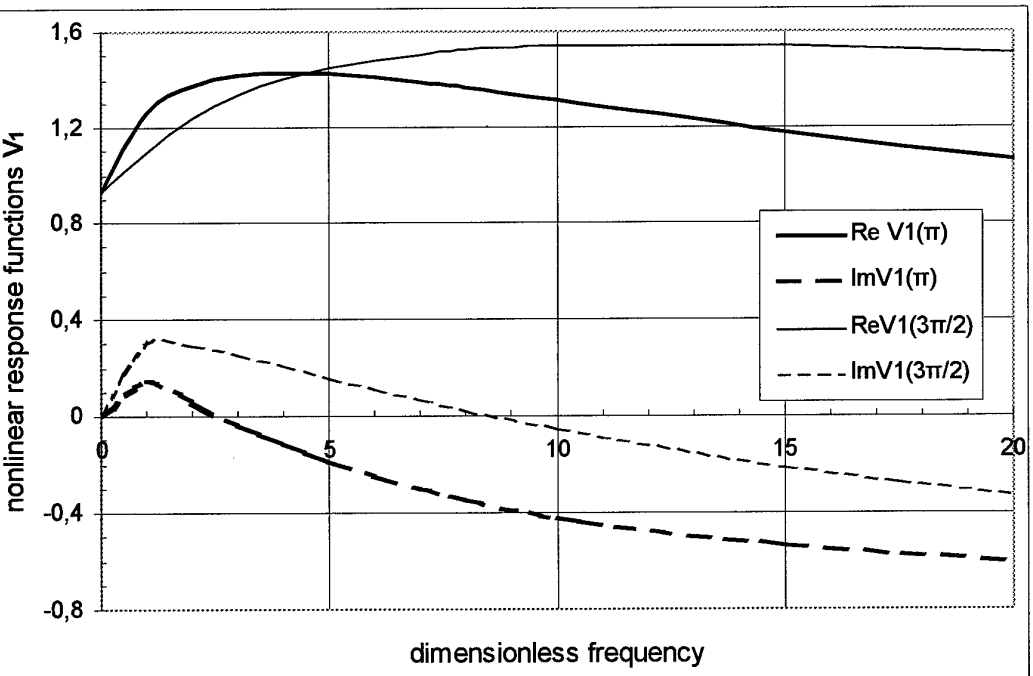

Figure 22: Nonlinear response functions **V1** of **GAP/HNIW**, at phase shift **ψ =π** and **ψ =3π/2**; p=**10** MPa,To=20'C

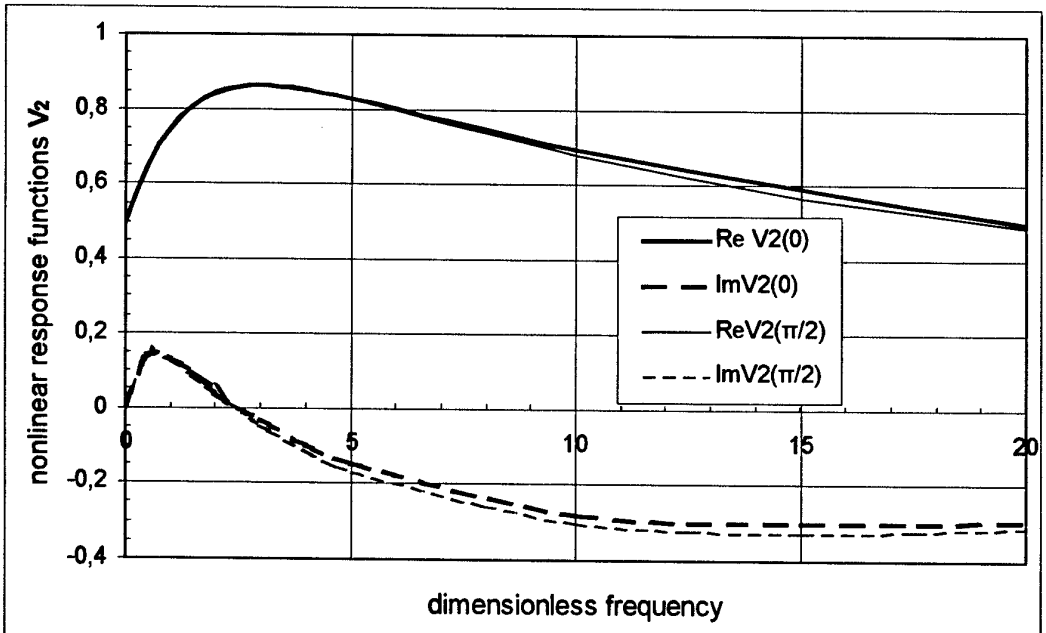

Figure 23: Nonlinear response functions **V2** (linear functions plus corrections by second order self-interaction of the first mode) of **GAP/HNIW,** at phase shift **ψ =0** and **ψ =π/2**; **p=0,5** MPa,To=20'C.

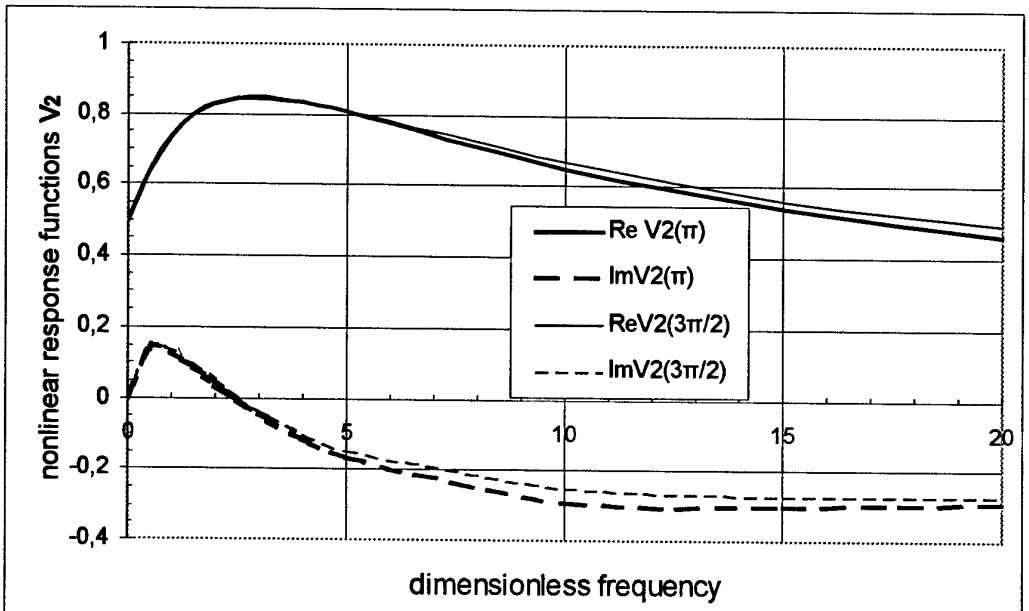

Figure 24: Nonlinear response functions **V2** of **GAP/HNIW,** at phase shift **ψ =π** and **ψ =3π/2**; **p=0,5** MPa,To=20'C.

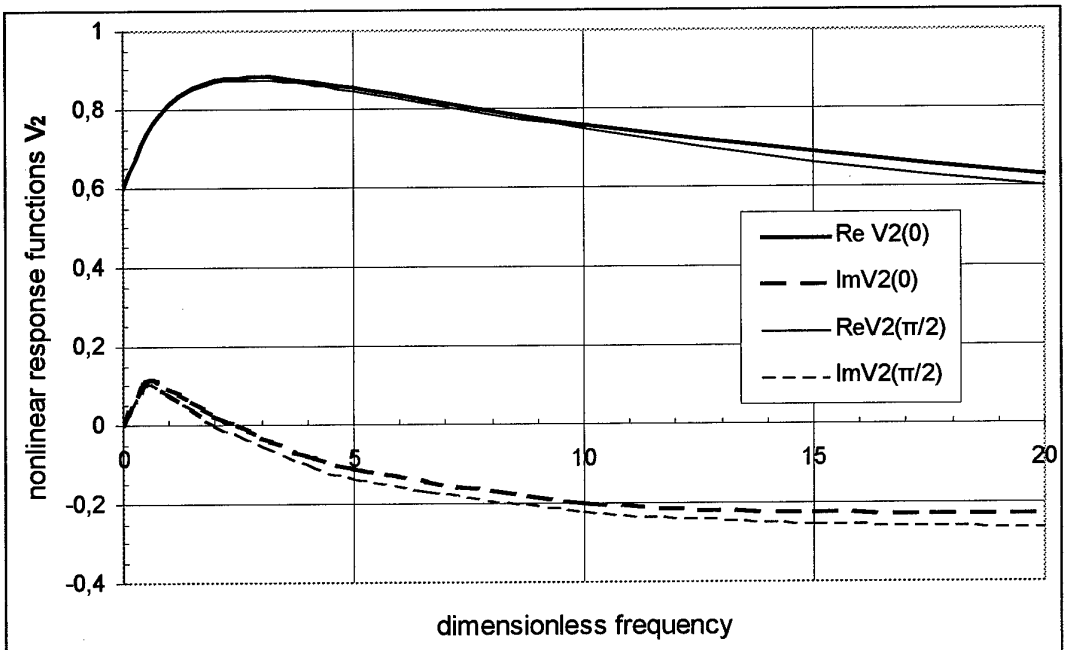

Figure 25: Nonlinear response functions V_2 (linear functions plus corrections by second order self-interaction of the first mode) of **GAP/HNIW,** at phase shift $\psi = 0$ and $\psi = \pi/2$; p=1 MPa,To=20'C.

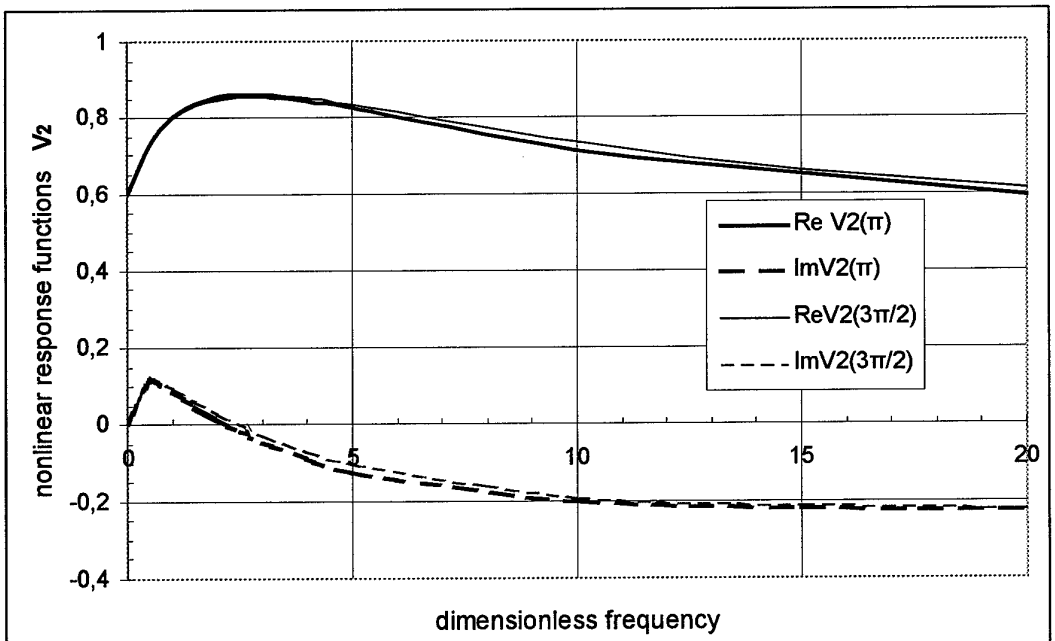

Figure 26: Nonlinear response functions V_2 of **GAP/HNIW,** at phase shift $\psi = \pi$ and $\psi = 3\pi/2$; p=1 MPa,To=20'C.

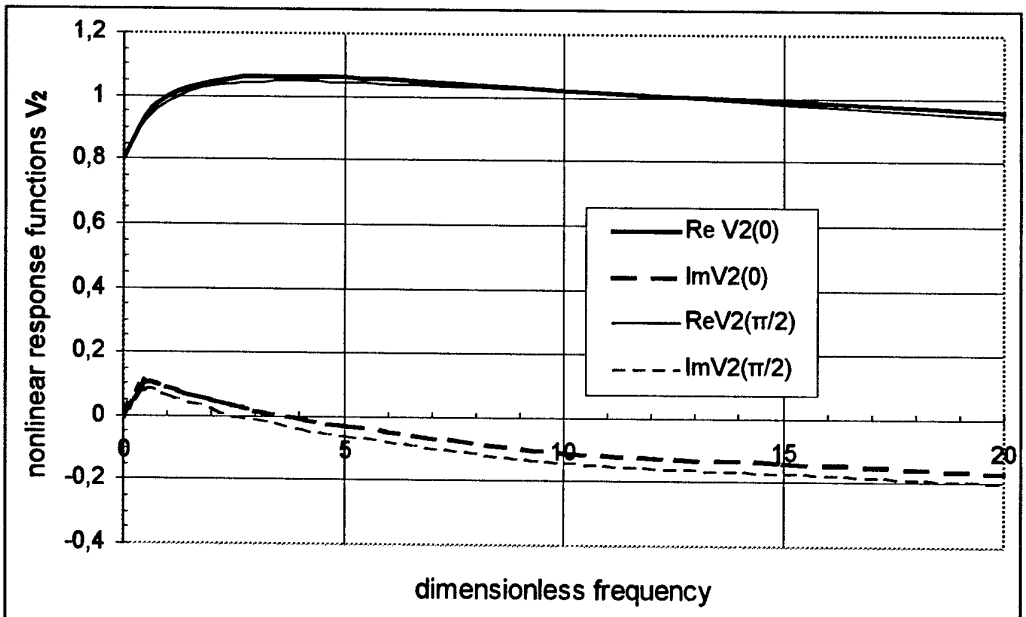

Figure 27: Nonlinear response functions V_2 (linear functions plus corrections by second order self-interaction of the first mode) of **GAP/HNIW,** at phase shift $\psi = 0$ and $\psi = \pi/2$; p=5 MPa, To=20'C.

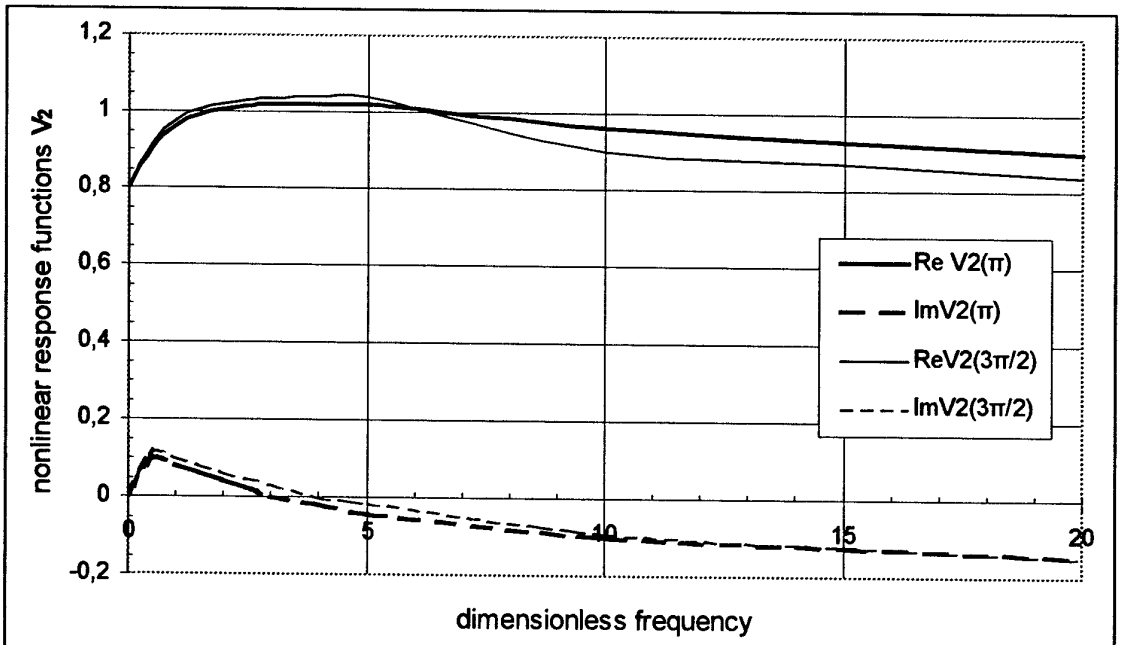

Figure 28: Nonlinear response functions V_2 of **GAP/HNIW,** at phase shift $\psi = \pi$ and $\psi = 3\pi/2$; p=5 MPa, To=20'C.

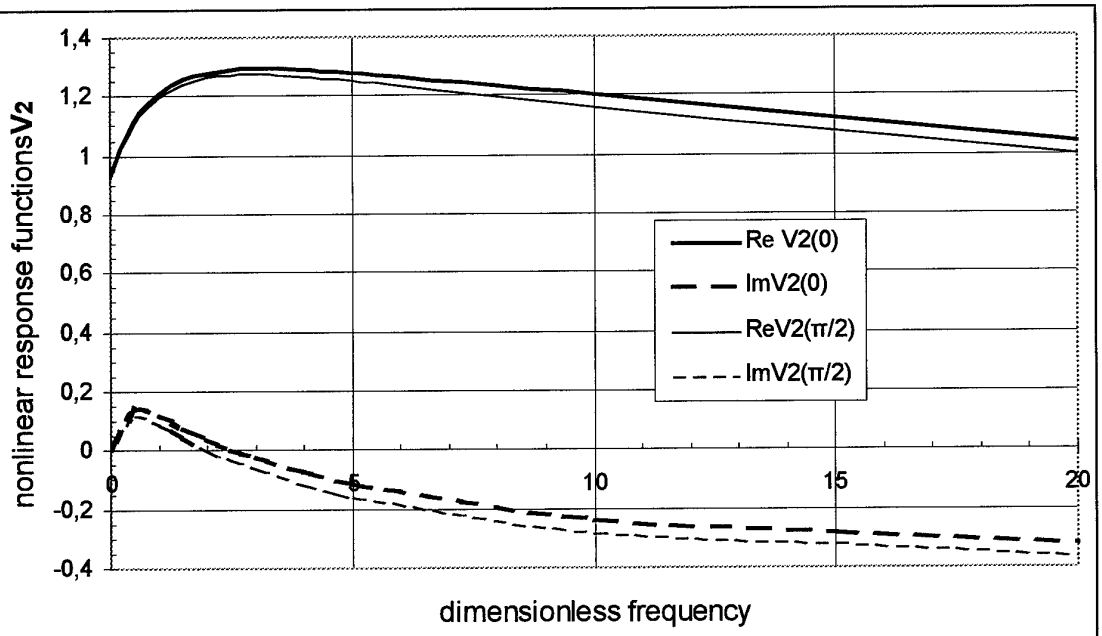

Figure 29: Nonlinear response functions V_2 (linear functions plus corrections by second order self-interaction of the first mode) of **GAP/HNIW**, at phase shift $\psi = 0$ and $\psi = \pi/2$; p=10 MPa, To=20'C.

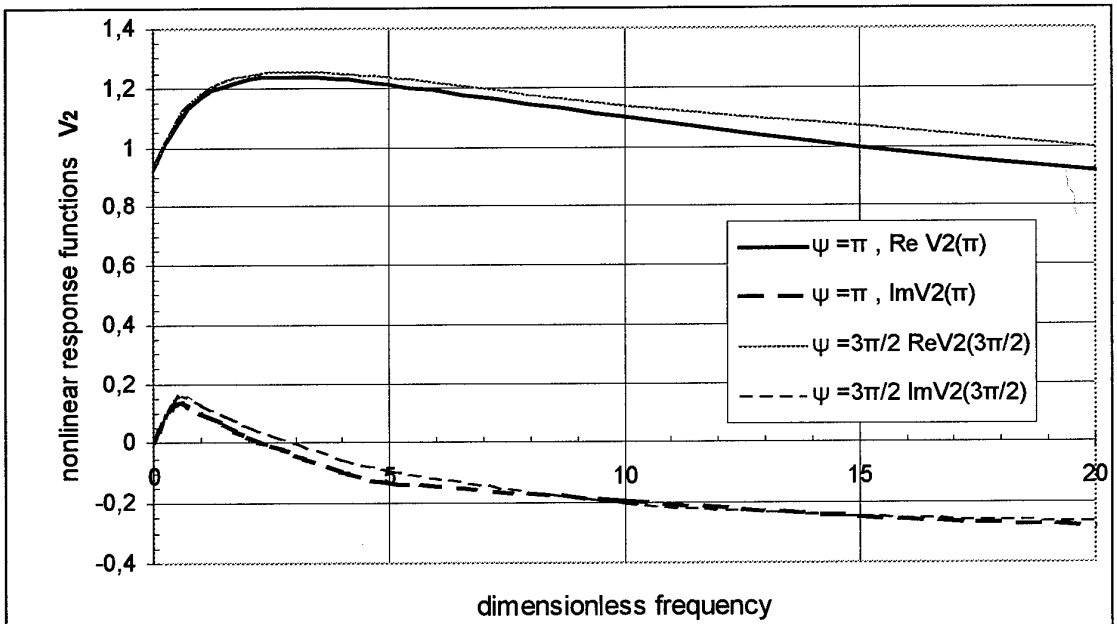

Figure 30: Nonlinear response functions V_2 of **GAP/HNIW**, at phase shift $\psi = \pi$ and $\psi = 3\pi/2$; p=10 MPa, To=20'C.